Designing Horndeski and the effective fluid approach

Rubén Arjona,* Wilmar Cardona,† and Savvas Nesseris‡

Instituto de Física Teórica UAM-CSIC, Universidad Autonóma de Madrid, Cantoblanco, 28049 Madrid, Spain

(Received 16 April 2019; published 20 September 2019)

We present a family of designer Horndeski models, i.e., models that have a background exactly equal to that of the ΛCDM model but perturbations given by the Horndeski theory. Then, we extend the effective fluid approach to Horndeski theories, providing simple analytic formulas for the equivalent dark energy effective fluid pressure, density, and velocity. We implement the dark energy effective fluid formulas in our code EFCLASS, a modified version of the widely used Boltzmann solver CLASS, and compare the solution of the perturbation equations with those of the code HI_CLASS which already includes Horndeski models. We find that our simple modifications to the VANILLA code are accurate to the level of ∼0.1% with respect to the more complicated HI_CLASS code. Furthermore, we study the kinetic braiding model both on and off the attractor, and we find that even though the full case has a proper ΛCDM limit for large n, it is not appropriately smooth, thus causing the quasistatic approximation to break down. Finally, we focus on our designer model (HDES), which has both a smooth ΛCDM limit and well-behaved perturbations, and we use it to perform Markov Chain–Monte Carlo analyses to constrain its parameters with the latest cosmological data. We find that our HDES model can also alleviate the soft 2σ tension between the growth data and Planck 18 due to a degeneracy between σ_8 and one of its model parameters that indicates the deviation from the ΛCDM model.

DOI: 10.1103/PhysRevD.100.063526

I. INTRODUCTION

Not long ago, measurements of the distance-redshift relation from distant Supernovae type Ia (SNIa) revealed that the Universe is not only expanding as time goes by, it is actually accelerating [1,2]. The consequences of these observations are far-reaching and several analyses of the datasets have been carefully carried out ever since (see Ref. [3] and references therein). Although there were some concerns about possible systematic errors, analyses of new and improved datasets have shown that results in previous works are robust [4,5]. Moreover, most recent astrophysical measurements of the cosmic microwave background (CMB) anisotropies and the distribution of galaxies in the Universe, when interpreted in the context of the cosmological constant cold dark matter model (ΛCDM), are in very good agreement with a late-time accelerating phase [6,7].

Current Bayesian analyses of astrophysical measurements indicate that ΛCDM beats alternative models [8]. In spite of being successful at fitting most datasets, ΛCDM is just a very good phenomenological model as its main constituents are either unknown or misunderstood. First, cold dark matter (CDM) has not been directly detected thus far despite the huge effort this research field has attracted over the past years [9]. Second, there exists an important disagreement between both predicted and inferred values of the cosmological constant Λ whose solution will possibly lead to new physics [10,11].

Even though reconciling the quantum field theory prediction with the observed value of the cosmological constant seems unlikely, it has become clear that a dark energy (DE) component resembling a cosmological constant not only can alleviate several problems present in a CDM model but also can drive the current accelerating expansion of the Universe [12]. Although several mechanisms have been proposed in the literature which could be responsible for speeding up the Universe, nowadays there are two main approaches. On the one hand, one finds modified gravity (MG) models [13]. Einstein's theory of general relativity (GR), the theory of gravity that is assumed in the ΛCDM model, seems to break down on tiny scales and possibly will require modifications on large scales to account for current observations [14]. However, modifying GR can be laborious as several tests carried out up to cosmological scales agree very well with GR [15–28]. On the other hand, there are DE models [29] which rely on yet unobserved scalar fields that would dominate the energy content of the Universe at late times and also avoid fine-tuning issues [30,31].

*ruben.arjona@uam.es
†wilmar.cardona@uam.es
‡savvas.nesseris@csic.es

 © 2019 American Physical Society

Although DE and MG models are clearly motivated by different underlying physics, it is possible to study both kinds of models on the same footing. In an effective fluid approach departures from GR can be interpreted as an effective fluid contribution in such a way that comparison with DE models might become relatively simple [32–36]. When interpreted as fluids, MG models can be described by an equation of state $w(a)$, a sound speed $c_s^2(a,k)$, and an anisotropic stress $\pi(a,k)$: background is affected by the behavior of $w(a)$ while perturbations are mainly governed by $c_s^2(a,k)$ and $\pi(a,k)$. Since both DE and MG models predict different behavior for these three functions, in an effective fluid approach different models can be, to a certain degree, distinguished.

It is well known that both DE and MG models can accommodate background astrophysical observations as well as the standard cosmological model ΛCDM [e.g., the so-called designer $f(R)$ models [37–40]]. As a consequence, these models are degenerated at the background level even though there have been various attempts to disentangle them by using model independent approaches [41,42]. Fortunately, the study of linear order perturbations might break this degeneracy because DE and MG models predict different growths of structures and could in principle be distinguishable from ΛCDM [39,43].

Given the wide range of both DE and MG models it is useful to have a unified framework which encompasses several of them. It turns out that such a theory exists since 1974 when Horndeski found the most general Lorentz-invariant extension of GR in four dimensions [44]. This theory can be obtained by using a single scalar field and restricting the equations of motion to being second order in time derivatives. The Horndeski Lagrangian comprehends theories such as kinetic gravity braiding, Brans-Dicke and scalar tensor gravity, single field quintessence, and K-essence theories, as well as $f(R)$ theories in their scalar-tensor formulation [45]. Although the range of models encompassed by the Horndeski Lagrangian was severely reduced (see, for instance, [46–58]) with the recent discovery of gravitational waves by the LIGO Collaboration [59], an interesting remaining subclass of models [including $f(R)$ theories [60–63] and kinetic gravity braiding [64]] is well worth an investigation.

Recently we employed an effective fluid approach to study $f(R)$ theories [65]. Even though it is not easy to obtain expressions for quantities describing perturbations (e.g., pressure perturbation δP) in MG models [66], by using the quasistatic and subhorizon approximations we found analytical expressions for the effective DE perturbations as well as the quantities describing the effective DE fluid, namely, $w(a)$, $c_s^2(a,k)$, and $\pi(a,k)$. We implemented our approach in the code CLASS[1] [67] and found excellent agreement with the so-called equation of state (EOS) approach [68,69], which does not use any approximation. In this paper we extend our work [65] to the remaining part of the Horndeski Lagrangian which contains $f(R)$ theories as a special case. Horndeski theories have been implemented in the code HI_CLASS [70] which solves the full set of dynamical equations without using the quasistatic approximation. In our approach we find analytical expressions for the effective DE perturbations that give us a better understanding of the underlying physics and also allow us to compare with our numerical implementation. Moreover, we show that it is possible to find "designer Horndeski theories" matching a given background evolution. We implement one such model in the HI_CLASS code and show there is good agreement with our approach; namely, our effective fluid approach assuming both quasistatic and subhorizon approximations performs quite well.

The paper is organized as follows. In Sec. II we discuss the equations for perturbations in a Friedmann-Lemaître-Robertson-Walker (FLRW) metric and set our notation. Then, we introduce the Horndeski Lagrangian and discuss both background and perturbation equations in Sec. III. In Sec. IV we study the remaining subclass of Horndeski theories by utilizing the effective fluid approach, we discuss the subhorizon and quasistatic approximations and present analytical results for two classes of models, those in which we have dark energy anisotropic stress and those in which we do not. In Sec. V we show analytical results for a family of models named "designer Horndeski" which mimic the ΛCDM background, and in Sec. VI we compare our analytical solutions for DE perturbations with a fully numerical solution of the system of differential equations and show they are in very good agreement. We then constrain the parameter space for a viable designer Horndeski model in Sec. VII, and in Sec. VIII we present our conclusions. In Appendixes A and B we give details about our analytical computations.

II. THEORETICAL FRAMEWORK

In the standard cosmological model one assumes the Einstein-Hilbert action

$$S = \int d^4x\sqrt{-g}\left[\frac{1}{2\kappa}R + \mathcal{L}_m\right], \tag{1}$$

where g is the determinant of the metric $g_{\mu\nu}$, R is the Ricci scalar, $\kappa \equiv \frac{8\pi G_N}{c^4}$, and $\mathcal{L}_m$ is the Lagrangian for matter fields.[2] Applying the principle of least action to Eq. (1) one obtains the field equations

[1] http://class-code.net/.

[2] Throughout this paper we set the speed of light $c = 1$ and $\kappa = 8\pi G_N$ with G_N being the bare Newton's constant. Our conventions are $(-+++)$ for the metric signature, and the Riemann and Ricci tensors are given, respectively, by $V_{b;cd} - V_{b;dc} = V_a R^a_{bcd}$ and $R_{ab} = R^s_{asb}$.

$$G_{\mu\nu} = \kappa T^{(m)}_{\mu\nu}, \tag{2}$$

where $G_{\mu\nu} \equiv R_{\mu\nu} - \frac{1}{2} g_{\mu\nu} R$ is the Einstein tensor and $T^{(m)}_{\mu\nu}$ is the energy-momentum tensor for matter fields. At this point one needs to make more assumptions about the geometrical properties and the matter content in the Universe. First, since observations indicate the Universe on large scales is statistically homogeneous and isotropic [71,72] (also having tiny inhomogeneities which can be treated within linear perturbation theory), one further assumes a perturbed FLRW metric

$$ds^2 = -(1 + 2\Psi(\vec{x}, t))dt^2 + a(t)^2(1 + 2\Phi(\vec{x}, t))d\vec{x}^2, \tag{3}$$

where a is the scale factor, $\vec{x}$ represents spatial coordinates, t is the cosmic time, and Ψ and Φ are the gravitational potentials in the Newtonian gauge. Second, one can suppose the matter fields are ideal fluids (with small perturbations) having an energy-momentum tensor given by

$$T^{\mu}_{\nu} = P\delta^{\mu}_{\nu} + (\rho + P)U^{\mu}U_{\nu}, \tag{4}$$

where P is the pressure, ρ is the energy density, and $U^{\mu} = (1 - \Psi, \frac{\vec{u}}{a(t)})$ is the velocity four-vector. As a result, the elements of the energy-momentum tensor up to first order are given by

$$T^0_0 = -(\bar{\rho} + \delta\rho), \tag{5}$$

$$T^0_i = (\bar{\rho} + \bar{P})a(t)u_i, \tag{6}$$

$$T^i_j = (\bar{P} + \delta P)\delta^i_j + \Sigma^i_j, \tag{7}$$

where $\bar{\rho}$ is the background energy density, $\bar{P}$ is the background pressure, $u_i = a(t)\dot{x_i}$, $\Sigma^i_j(\vec{x}, \tau) \equiv T^i_j - \delta^i_j T^k_k/3$ is an anisotropic stress tensor, and $\delta\rho(\vec{x}, \tau)$ and $\delta P(\vec{x}, \tau)$ are the density and pressure perturbations, respectively.[3]

A. Background

If one only considers zero order quantities in the Einstein field equations (2), then there are two independent Friedmann equations describing the background evolution of the Universe:

$$H^2 = \frac{\kappa}{3}\bar{\rho}, \tag{8}$$

$$H^2 + \dot{H} = -\frac{\kappa}{6}(\bar{\rho} + 3\bar{P}), \tag{9}$$

where $H \equiv \frac{\dot{a}}{a}$ is the cosmic Hubble parameter.[4]

B. Linear perturbations

Considering just the first order perturbations in the Einstein field equations (2) we obtain

$$-\frac{k^2}{a^2}\Phi + 3\frac{\dot{a}}{a}\left(\frac{\dot{a}}{a}\Psi - \dot{\Phi}\right) = \frac{\kappa}{2}\delta T^0_0, \tag{10}$$

$$k^2\left(\frac{\dot{a}}{a}\Psi - \dot{\Phi}\right) = \frac{\kappa}{2}a(\bar{\rho} + \bar{P})\theta, \tag{11}$$

$$-\frac{k^2}{3a^2}(\Phi + \Psi) + \left(2\frac{\ddot{a}}{a} + \frac{\dot{a}^2}{a^2}\right)\Psi + \frac{\dot{a}}{a}(\dot{\Psi} - 3\dot{\Phi}) - \ddot{\Phi} = \frac{\kappa}{6}\delta T^i_i, \tag{12}$$

$$-k^2(\Phi + \Psi) = \frac{3\kappa}{2}a^2(\bar{\rho} + \bar{P})\sigma, \tag{13}$$

where we defined the velocity $\theta \equiv ik^j u_j$ and wrote the anisotropic stress as $(\bar{\rho} + \bar{P})\sigma \equiv -(\hat{k}_i\hat{k}_j - \frac{1}{3}\delta_{ij})\Sigma^{ij}$.

From the conservation of the energy-momentum tensor $T^{\mu\nu}_{;\nu} = 0$ one obtains the equations for the evolution of perturbations. Defining the equation of state parameter as $w \equiv \frac{\bar{P}}{\bar{\rho}}$ and the sound speed $c_s^2 \equiv \frac{\delta P}{\delta\rho}$ we find the equations governing the evolution of density and pressure perturbations are given by

$$\dot{\delta} = -(1 + w)\left(\frac{\theta}{a} + 3\dot{\Phi}\right) - 3\frac{\dot{a}}{a}(c_s^2 - w)\delta, \tag{14}$$

$$\dot{\theta} = -\frac{\dot{a}}{a}(1 - 3w)\theta - \frac{\dot{w}}{1 + w}\theta + \frac{c_s^2}{1 + w}\frac{k^2}{a}\delta - \frac{k^2}{a}\sigma + \frac{k^2}{a}\Psi. \tag{15}$$

The system of differential equations (14) and (15) presents problems when the equation of state crosses -1 because there is a singularity. However, a simple change of variable turns out to be helpful in solving this inconvenience. We will use the scalar velocity perturbation $V \equiv ik_j T^j_0/\rho = (1 + w)\theta$ instead of the velocity θ. In terms of this new variable the evolution equations (14) and (15) become

$$\delta' = -3(1 + w)\Phi' - \frac{V}{a^2 H} - \frac{3}{a}\left(\frac{\delta P}{\bar{\rho}} - w\delta\right), \tag{16}$$

[3]In our notation, a dot over a function f denotes the derivative with respect to the cosmic time: $\dot{f} \equiv \frac{df}{dt}$. In addition, Greek indices run from 0 to 3, whereas Latin indices take on values from 1 to 3.

[4]The conformal Hubble parameter $\mathcal{H}$ and the Hubble parameter H are related via $\mathcal{H} = aH$.

$$V' = -(1-3w)\frac{V}{a} + \frac{k^2}{a^2H}\frac{\delta P}{\bar{\rho}} + (1+w)\frac{k^2}{a^2H}\Psi - \frac{2}{3}\frac{k^2}{a^2H}\pi, \tag{17}$$

where a prime $'$ denotes a derivative with respect to the scale factor and we defined the anisotropic stress parameter $\pi \equiv \frac{3}{2}(1+w)\sigma$.

III. HORNDESKI

Horndeski theory constitutes the most general Lorentz-invariant extension of GR in four dimensions and encompasses several DE and MG models. Although in its most general form the Horndeski Lagrangian has several free functions, the recent discovery of gravitational waves by the LIGO Collaboration significantly constrained the allowed models. In particular, it has been shown that the constraint on the speed of gravitational waves must satisfy [48]

$$-3\times 10^{-15} \leq c_g/c - 1 \leq 7\times 10^{-16}, \tag{18}$$

which for Horndeski theories implies that

$$G_{4X} \approx 0, \qquad G_5 \approx \text{const}, \tag{19}$$

as can be seen from the sound speed formula for tensor perturbations [73]

$$c_T^2 = \frac{G_4 - XG_{5\phi} - XG_{5X}\ddot{\phi}}{G_4 - 2XG_{4X} - X(G_{5X}\dot{\phi}H - G_{5\phi})}. \tag{20}$$

In this section we will derive evolution equations for the remaining parts of the Horndeski Lagrangian, namely,

$$S[g_{\mu\nu},\phi] = \int d^4x\sqrt{-g}\left[\sum_{i=2}^{4}\mathcal{L}_i[g_{\mu\nu},\phi] + \mathcal{L}_m\right], \tag{21}$$

where

$$\mathcal{L}_2 = G_2(\phi,X) \equiv K(\phi,X), \tag{22}$$

$$\mathcal{L}_3 = -G_3(\phi,X)\Box\phi, \tag{23}$$

$$\mathcal{L}_4 = G_4(\phi)R. \tag{24}$$

Here ϕ is a scalar field, $X \equiv -\frac{1}{2}\partial_\mu\phi\partial^\mu\phi$ is a kinetic term, and $\Box\phi \equiv g^{\mu\nu}\nabla_\mu\nabla_\nu\phi$; K, G_3, and G_4 are free functions of ϕ and X.[5] Since we are mainly interested in the late-time dynamics of the Universe, hereafter we will further assume $\mathcal{L}_m$ is the Lagrangian of a CDM component. As has been mentioned in [52], although the functions K, G_3, and G_4 are able to modify the background with a general dependence on X and ϕ, this does not hold at the perturbations level. For instance, $K(\phi,X)$ encloses the k-essence and quintessence theory and is partly responsible for the background and the perturbations; however, $K(\phi)$ does not contribute to the perturbations.

The term $G_3(\phi,X)$ includes the kinetic gravity braiding with $G_{3X} \neq 0$ being in charge of combining the kinetic term of the scalar and the metric, but the term $G_3(\phi)$ only modifies the background as a dynamical dark energy. Finally, G_4 is the only function that is able to modify the nonminimal coupling of the scalar to the Ricci curvature.

Among the theories embedded in the action (21) one finds, for example,

(i) *f(R) theories.* When interpreted as a nonminimal coupled scalar field, these theories can be written using [74]

$$K = -\frac{Rf_{,R} - f}{2\kappa}, \tag{25}$$

$$G_4 = \frac{\phi}{2\sqrt{\kappa}}, \tag{26}$$

where $\phi \equiv \frac{f_{,R}}{\sqrt{\kappa}}$ has units of mass and $f_{,R} \equiv \frac{df}{dR}$.

(ii) *Brans-Dicke theories.* In our notation we have

$$K = \frac{\omega_{\rm BD}X}{\phi\sqrt{\kappa}} - V(\phi), \tag{27}$$

$$G_4 = \frac{\phi}{2\sqrt{\kappa}}, \tag{28}$$

where $V(\phi)$ is the field potential and $\omega_{\rm BD}$ is the Brans-Dicke parameter [75].

(iii) *Kinetic gravity braiding.* This kind of scalar-tensor models exhibit mixing of scalar and tensor kinetic terms [64] and can be written as

$$K = K(X), \tag{29}$$

$$G_3 = G_3(X), \tag{30}$$

$$G_4 = \frac{1}{2\kappa}. \tag{31}$$

(iv) *Nonminimal coupling (NMC) model* [76]. In our notation and for a coupling constant ζ

$$K = \omega(\phi)X - V(\phi), \tag{32}$$

$$G_4 = \left(\frac{1}{2\kappa} - \frac{\zeta\phi^2}{2}\right), \tag{33}$$

[5]From now on we define $G_i \equiv G_i(\phi,X)$, $G_{i,X} \equiv G_{iX} \equiv \frac{\partial G_i}{\partial X}$, and $G_{i,\phi} \equiv G_{i\phi} \equiv \frac{\partial G_i}{\partial \phi}$ where $i = 2, 3, 4$.

$$G_3 = 0. \tag{34}$$

In the context of inflation, a Higgs-like inflation model corresponds to $\omega(\phi) = 1$, $V(\phi) = \lambda(\phi^2 - \nu^2)^2/4$.

(v) *Cubic Galileon* [76]. The simplest case is when

$$K = -X, \tag{35}$$

$$G_3 \propto X, \tag{36}$$

$$G_4 = \frac{1}{2\kappa}. \tag{37}$$

(vi) *Four-dimensional static and spherical symmetric solution of black hole with scalar hair* [77].

$$K = X, \tag{38}$$

$$G_3 = -\frac{\alpha \log(-X)}{\sqrt{\kappa}}, \tag{39}$$

$$G_4 = \frac{1}{2\kappa}. \tag{40}$$

As previously done for the Einstein-Hilbert action (1), here we apply the principle of least action to (21) in order to find evolution equations for both the gravitational field and the scalar field. Varying Eq. (21) with respect to the metric and the scalar field one finds[6] [73]

$$\delta\left(\sqrt{-g}\sum_{i=2}^{4}\mathcal{L}_i\right) = \sqrt{-g}\left[\sum_{i=2}^{4}\mathcal{G}^i_{\mu\nu}\delta g^{\mu\nu} + \sum_{i=2}^{4}(P^i_\phi - \nabla^\mu J^i_\mu)\delta\phi\right] + \text{total derivative}, \tag{41}$$

which allows us to find the field equations. First, the gravitational field equation is given by

$$\sum_{i=2}^{4}\mathcal{G}^i_{\mu\nu} = \frac{1}{2}T^{(m)}_{\mu\nu}, \tag{42}$$

where we have defined

$$\mathcal{G}^2_{\mu\nu} = -\frac{1}{2}K_X\nabla_\mu\phi\nabla_\nu\phi - \frac{1}{2}Kg_{\mu\nu}, \tag{43}$$

$$\mathcal{G}^3_{\mu\nu} = \frac{1}{2}G_{3X}\Box\phi\nabla_\mu\phi\nabla_\nu\phi + \nabla_{(\mu}G_3\nabla_{\nu)}\phi - \frac{1}{2}g_{\mu\nu}\nabla_\lambda G_3\nabla^\lambda\phi, \tag{44}$$

$$\mathcal{G}^4_{\mu\nu} = G_4G_{\mu\nu} + g_{\mu\nu}(G_{4\phi}\Box\phi - 2XG_{4\phi\phi}) - G_{4\phi}\nabla_\mu\nabla_\nu\phi - G_{4\phi\phi}\nabla_\mu\phi\nabla_\nu\phi, \tag{45}$$

and $T^{(m)}_{\mu\nu}$ is the energy-momentum tensor of a CDM component. Note that from Eq. (42) we retrieve the GR field equations (2) if we set $K = G_3 = 0$ and $G_4 = \frac{1}{2\kappa}$. Second, the scalar field equation reads

$$\nabla^\mu\left(\sum_{i=2}^{4}J^i_\mu\right) = \sum_{i=2}^{4}P^i_\phi, \tag{46}$$

where

$$P^2_\phi = K_\phi, \tag{47}$$

$$P^3_\phi = \nabla_\mu G_{3\phi}\nabla^\mu\phi, \tag{48}$$

$$P^4_\phi = G_{4\phi}R, \tag{49}$$

$$J^2_\mu = -\mathcal{L}_{2X}\nabla_\mu\phi, \tag{50}$$

$$J^3_\mu = -\mathcal{L}_{3X}\nabla_\mu\phi + G_{3X}\nabla_\mu X + 2G_{3\phi}\nabla_\mu\phi, \tag{51}$$

$$J^4_\mu = 0. \tag{52}$$

As it is mentioned in Ref. [73], one could think $\nabla^\mu J^i_\mu$ leads to higher than second-order derivatives. However, this is not the case since commutations of higher derivatives can be substituted by the curvature tensor and are hence canceled. In particular, one can prove that

$$\nabla_\mu(\Box\phi\nabla^\mu\phi + \nabla^\mu X) = (\Box\phi)^2 - (\nabla_\alpha\nabla_\beta\phi)^2 - R_{\mu\nu}\nabla^\mu\phi\nabla^\nu\phi, \tag{53}$$

which will be of paramount importance when we will discuss perturbation equations.

It is possible to find a relatively simple expression for the scalar field equation (46) if we consider the case $i = 3$, namely,

$$0 = 2G_{3\phi}\Box\phi + \nabla^\mu G_{3\phi}\nabla_\mu\phi + \nabla_\mu\phi\nabla^\mu G_{3X}\Box\phi + \underbrace{\nabla^\mu(G_{3X}\nabla_\mu X) + G_{3X}(\Box\phi)^2 + G_{3X}\nabla_\mu\phi\nabla^\mu\Box\phi}. \tag{54}$$

The terms on top of the brace in Eq. (54) can be expanded as

$$\nabla^\mu G_{3X}\nabla_\mu X + \underbrace{G_{3X}\Box X + G_{3X}(\Box\phi)^2 + G_{3X}\nabla^\mu\phi\nabla_\mu\Box\phi} = 0, \tag{55}$$

[6]See Appendix A for a derivation of the field equations.

and the terms on top of the brace in Eq. (55) can in turn be written as

$$G_{3X}[\nabla^\mu\phi\nabla_\mu\Box\phi + (\Box\phi)^2 + \Box X] = G_{3X}[\nabla_\mu(\Box\phi\nabla^\mu\phi + \nabla^\mu X)]. \tag{56}$$

Using Eq. (53) in Eq. (56) we find

$$G_{3X}[\nabla^\mu\phi\nabla_\mu\Box\phi + (\Box\phi)^2 + \Box X] = G_{3X}[(\Box\phi)^2 - (\nabla_\alpha\nabla_\beta\phi)^2 - R_{\mu\nu}\nabla^\mu\phi\nabla^\nu\phi], \tag{57}$$

and the scalar field equation (46) can be written as

$$-\nabla_\mu K_X\nabla^\mu\phi - K_X\Box\phi - K_\phi + 2G_{3\phi}\Box\phi + \nabla_\mu G_{3\phi}\nabla^\mu\phi + \nabla_\mu G_{3X}\Box\phi\nabla^\mu\phi + \nabla_\mu G_{3X}\nabla^\mu X + G_{3X}[(\Box\phi)^2 - (\nabla_\alpha\nabla_\beta\phi)^2 - R_{\mu\nu}\nabla^\mu\phi\nabla^\nu\phi] - G_{4\phi}R = 0. \tag{58}$$

In what follows, in order to simplify the notation we will denote the kinetic term of the scalar field evaluated at the background simply by X and its linear order perturbation as δX.

A. Background

Thus far the discussion of the field equations has been quite general. Now, as previously done in Sec. II, we assume a perturbed FLRW as given in Eq. (3). If we consider only zero order quantities in the gravitational field equation (42), we obtain

$$\mathcal{E} \equiv \sum_{i=2}^{4}\mathcal{E}_i = -\rho_m, \tag{59}$$

$$\mathcal{P} \equiv \sum_{i=2}^{4}\mathcal{P}_i = 0, \tag{60}$$

where

$$\mathcal{E}_2 \equiv 2XK_X - K, \tag{61}$$

$$\mathcal{E}_3 \equiv 6X\dot\phi HG_{3X} - 2XG_{3\phi}, \tag{62}$$

$$\mathcal{E}_4 \equiv -6H^2G_4 - 6H\dot\phi G_{4\phi}, \tag{63}$$

$$\mathcal{P}_2 \equiv K, \tag{64}$$

$$\mathcal{P}_3 \equiv -2X(G_{3\phi} + \ddot\phi G_{3X}), \tag{65}$$

$$\mathcal{P}_4 \equiv 2(3H^2 + 2\dot H)G_4 + 2(\ddot\phi + 2H\dot\phi)G_{4\phi} + 2\dot\phi^2G_{4\phi\phi}. \tag{66}$$

Equations (59) and (60) are the modified Friedmann equations describing the background evolution of the Universe. Collecting terms they, respectively, read

$$2XK_X - K + 6X\dot\phi HG_{3X} - 2XG_{3\phi} - 6H^2G_4 - 6H\dot\phi G_{4\phi} + \rho_m = 0, \tag{67}$$

$$K - 2X(G_{3\phi} + \ddot\phi G_{3X}) + 2(3H^2 + 2\dot H)G_4 + 2(\ddot\phi + 2H\dot\phi)G_{4\phi} + 2\dot\phi^2G_{4\phi\phi} = 0. \tag{68}$$

Note that from Eqs. (67) and (68) we, respectively, retrieve the Friedmann equations (8) and (9) if we set $K = G_3 = 0$ and $G_4 = \frac{1}{2\kappa}$. Rearranging terms in Eqs. (67) and (68) we can define an effective DE density

$$\bar\rho_{\rm DE} = \dot\phi^2K_X - K + 3\dot\phi^3HG_{3X} - \dot\phi^2G_{3\phi} + 3H^2\left(\frac{1}{\kappa} - 2G_4\right) - 6H\dot\phi G_{4\phi}, \tag{69}$$

and an effective DE pressure

$$\bar P_{\rm DE} = K - \dot\phi^2(G_{3\phi} + \ddot\phi G_{3X}) + 2\dot\phi^2G_{4\phi\phi} + 2(\ddot\phi + 2H\dot\phi)G_{4\phi} - (3H^2 + 2\dot H)\left(\frac{1}{\kappa} - 2G_4\right), \tag{70}$$

in such a way that we can write the modified Friedmann equations (67) and (68) as

$$3H^2 = \kappa(\bar\rho_{\rm DE} + \rho_m), \tag{71}$$

$$-(2\dot H + 3H^2) = \kappa\bar P_{\rm DE}, \tag{72}$$

where we are assuming that matter is pressureless $\bar P_m = 0$ as indicated by current constraints [78]. The effective DE density and pressure in Eqs. (69) and (70) allow us to define an effective DE equation of state as

$$w_{\rm DE} = \frac{K - \dot\phi^2(G_{3\phi} + \ddot\phi G_{3X}) - (3H^2 + 2\dot H)(\frac{1}{\kappa} - 2G_4) + 2(\ddot\phi + 2H\dot\phi)G_{4\phi} + 2\dot\phi^2G_{4\phi\phi}}{\dot\phi^2K_X - K + 3\dot\phi^3HG_{3X} - \dot\phi^2G_{3\phi} + 3H^2(\frac{1}{\kappa} - 2G_4) - 6H\dot\phi G_{4\phi}}. \tag{73}$$

Let us now consider the scalar field equation (58) and only keep zero order quantities; that is to say,

$$K_\phi - (K_X - 2G_{3\phi})(\ddot{\phi} + 3H\dot{\phi}) - K_{\phi X}\dot{\phi}^2 - K_{XX}\ddot{\phi}\dot{\phi}^2 + G_{3\phi\phi}\dot{\phi}^2 + G_{3\phi X}\dot{\phi}^2(\ddot{\phi} - 3H\dot{\phi}) - 3G_{3X}(2H\dot{\phi}\ddot{\phi} + 3H^2\dot{\phi}^2 + \dot{H}\dot{\phi}^2) - 3G_{3XX}H\dot{\phi}^3\ddot{\phi} + 6G_{4\phi}(2H^2 + \dot{H}) = 0, \tag{74}$$

which fully agrees with [79]. Note that defining

$$J_\mu \equiv \sum_{i=2}^{4} J_\mu^i, \tag{75}$$

$$P_\phi \equiv \sum_{i=2}^{4} P_\phi^i, \tag{76}$$

we can write the scalar field equation (46) as

$$\nabla_\mu J^\mu = P_\phi, \tag{77}$$

and it becomes clear that there exists a Noether current for Lagrangians invariant under constant shifts of the field $\phi \to \phi + c$ [64], namely,

$$J_\mu = (\mathcal{L}_{2X} + \mathcal{L}_{3X} - 2G_{3\phi})\nabla_\mu\phi - G_{3X}\nabla_\mu X. \tag{78}$$

Taking into consideration that $X = \frac{1}{2}\dot{\phi}^2$, the charge density of the Noether current can be written as

$$J \equiv J_0 = \dot{\phi}(K_X - 2G_{3\phi} + 3H\dot{\phi}G_{3X}), \tag{79}$$

so that the scalar field equation is given by the simple expression

$$\dot{J} + 3HJ = P_\phi. \tag{80}$$

When $P_\phi = 0$, then it is easy to see that the solution to the previous equation is

$$J = \frac{J_c}{a^3}, \tag{81}$$

where J_c is a constant. When $J_c = 0$, then the system is on the attractor solution, but when $J_c \neq 0$, then the system is not on the attractor and, as we will see in Sec. IV B 3, interesting dynamics may arise.

B. Linear perturbations

Considering only first order quantities in the gravitational field equations (42) one obtains [80,81]

$$A_1\dot{\Phi} + A_2\delta\dot{\phi} + A_3\frac{k^2}{a^2}\Phi + A_4\Psi + \left(A_6\frac{k^2}{a^2} - \mu\right)\delta\phi - \rho_m\delta_m = 0, \tag{82}$$

$$C_1\dot{\Phi} + C_2\delta\dot{\phi} + C_3\Psi + C_4\delta\phi - \frac{a\rho_m V_m}{k^2} = 0, \tag{83}$$

$$B_1\ddot{\Phi} + B_2\delta\ddot{\phi} + B_3\dot{\Phi} + B_4\delta\dot{\phi} + B_5\dot{\Psi} + B_6\frac{k^2}{a^2}\Phi + \left(B_7\frac{k^2}{a^2} + 3\nu\right)\delta\phi + \left(B_8\frac{k^2}{a^2} + B_9\right)\Psi = 0, \tag{84}$$

$$G_4(\Psi + \Phi) + G_{4\phi}\delta\phi = 0. \tag{85}$$

Note that when $K = G_3 = 0$ and $G_4 = \frac{1}{2\kappa}$, Eqs. (82)–(85), respectively, correspond to the GR limit given by Eqs. (10)–(13) with $\sigma_m = 0$.

If we now consider the scalar field equation (58) and take into account only first order quantities, we find

$$D_1\ddot{\Phi} + D_2\delta\ddot{\phi} + D_3\dot{\Phi} + D_4\delta\dot{\phi} + D_5\dot{\Psi} + \left(D_7\frac{k^2}{a^2} + D_8\right)\Phi + \left(D_9\frac{k^2}{a^2} - M^2\right)\delta\phi + \left(D_{10}\frac{k^2}{a^2} + D_{11}\right)\Psi = 0. \tag{86}$$

Expressions for the coefficients A_i, μ, ν, B_i, C_i, and D_i can be found in Appendix B and are in agreement with those found in [80,81], except for D_8 which is actually equal to zero as can be seen by using the expression found in [81] and using the background equations of motion for the scalar field.

IV. THE EFFECTIVE FLUID APPROACH

We have seen in the previous section that the gravitational field equations for the Horndeski Lagrangian can be written in such a way that they resemble those found in Sec. II where we assumed GR and a perfect fluid. Indeed, defining an effective DE density and pressure given by Eqs. (69) and (70) makes it possible to obtain an effective DE equation of state [see Eq. (73)]. As mentioned in Sec. I, a fluid can be described by its equation of state, sound speed, and anisotropic stress, so in what follows we will explicitly derive those quantities.

In this section we will present relatively simple expressions for the effective DE sound speed and anisotropic stress under the subhorizon and quasistatic approximations. Actually, by defining an effective DE fluid we are considering a DE effective energy-momentum tensor $T_{\mu\nu}^{\rm DE}$ obtained via the gravitational field equations (42) and defined explicitly as follows:

$$G_{\mu\nu} = \kappa\left(T^{(m)}_{\mu\nu} + T^{(\mathrm{DE})}_{\mu\nu}\right),$$
$$\kappa T^{(\mathrm{DE})}_{\mu\nu} = G_{\mu\nu} - 2\kappa\sum_{i=2}^{4}\mathcal{G}^{i}_{\mu\nu}. \tag{87}$$

Since we are taking into consideration expressions up to linear order, $T^{\mathrm{DE}}_{\mu\nu}$ also contains small perturbations which allow us to define quantities such as DE effective perturbations in the pressure, density, and velocity. These can be extracted from the DE effective energy-momentum tensor $T^{\mathrm{DE}}_{\mu\nu}$ by considering the decomposition of the tensor into its components, given by Eqs. (5)–(7). Qualitatively, these expressions have the following structure:

$$\frac{\delta P_{\mathrm{DE}}}{\bar{\rho}_{\mathrm{DE}}} = (\cdots)\delta\phi + (\cdots)\delta\dot{\phi} + (\cdots)\delta\ddot{\phi} + (\cdots)\Psi + (\cdots)\dot{\Psi} + (\cdots)\Phi + (\cdots)\dot{\Phi} + (\cdots)\ddot{\Phi}, \tag{88}$$

$$\delta_{\mathrm{DE}} = (\cdots)\delta\phi + (\cdots)\delta\dot{\phi} + (\cdots)\Psi + (\cdots)\Phi + (\cdots)\dot{\Phi}, \tag{89}$$

$$V_{\mathrm{DE}} = (\cdots)\delta\phi + (\cdots)\delta\dot{\phi} + (\cdots)\Psi + (\cdots)\Phi + (\cdots)\dot{\Phi}, \tag{90}$$

where $(\cdots)$ indicates expressions which might be cumbersome. It is therefore very helpful to work out these expressions under the subhorizon and quasistatic approximations in order to gain a better understanding.

We have explained in great detail the way we carry out the subhorizon and quasistatic approximations in our previous paper (see Sec. II.A.1 in Ref. [65]), but in a nutshell, the former refers to only considering modes deep in the Hubble radius, i.e., those for which $k^2 \gg a^2H^2$, while the latter refers to neglecting derivatives of the potentials during matter domination as they are roughly constant but also terms of similar order as $\partial_\eta \sim 1/\eta \sim aH(a)$. For example, the perturbation in the Ricci scalar is

$$\delta R = -\frac{12(\mathcal{H}^2 + \dot{\mathcal{H}})}{a^2}\Psi - \frac{4k^2}{a^2}\Phi + \frac{2k^2}{a^2}\Psi - \frac{18\mathcal{H}}{a^2}\dot{\Phi} - \frac{6\mathcal{H}}{a^2}\dot{\Psi} - \frac{6\ddot{\Phi}}{a^2} \simeq -\frac{4k^2}{a^2}\Phi + \frac{2k^2}{a^2}\Psi.$$

Following the same procedure and applying the subhorizon approximation to the linearized gravitational field equations (82) and (84), and to the linearized scalar field equation (86), one finds, respectively,

$$A_3\frac{k^2}{a^2}\Phi + A_6\frac{k^2}{a^2}\delta\phi - \kappa\rho_m\delta_m \simeq 0, \tag{91}$$

$$B_6\frac{k^2}{a^2}\Phi + B_8\frac{k^2}{a^2}\Psi + B_7\frac{k^2}{a^2}\delta\phi \simeq 0, \tag{92}$$

$$D_7\frac{k^2}{a^2}\Phi + \left(D_9\frac{k^2}{a^2} - M^2\right)\delta\phi + D_{10}\frac{k^2}{a^2}\Psi \simeq 0. \tag{93}$$

Note that since $B_7 = 4G_{4\phi}$ and $B_6 = B_8$ (see Appendix B), Eq. (92) leads to no anisotropic stress $\Phi = -\Psi$ when G_4 is a constant.

Solving Eqs. (91)–(93) for Φ, Ψ, and $\delta\phi$ one finds

$$\frac{k^2}{a^2}\Psi = -\frac{\kappa}{2}\frac{G_{\mathrm{eff}}}{G_N}\bar{\rho}_m\delta, \tag{94}$$

$$\frac{k^2}{a^2}\Phi = \frac{\kappa}{2}Q_{\mathrm{eff}}\bar{\rho}_m\delta, \tag{95}$$

$$\delta\phi = \frac{(A_6B_6 - B_6B_7)\rho_m\delta_m}{(A_6^2B_6 - 2A_6B_6B_7 + B_6^2D_9)\frac{k^2}{a^2} - B_6^2M^2}, \tag{96}$$

where G_{eff} and Q_{eff} are Newton's effective constant

$$\frac{G_{\mathrm{eff}}}{G_N} = \frac{2[(B_6D_9 - B_7^2)\frac{k^2}{a^2} - B_6M^2]}{(A_6^2B_6 + B_6^2D_9 - 2A_6B_7B_6)\frac{k^2}{a^2} - B_6^2M^2}, \tag{97}$$

$$Q_{\mathrm{eff}} = \frac{2[(A_6B_7 - B_6D_9)\frac{k^2}{a^2} + B_6M^2]}{(A_6^2B_6 + B_6^2D_9 - 2A_6B_7B_6)\frac{k^2}{a^2} - B_6^2M^2}, \tag{98}$$

and we make use of the following correspondence $A_3 = B_6 = B_8$, $D_7 = B_7$, and $D_{10} = A_6$ (see Appendix B). One can also define the following anisotropic stress parameters:

$$\eta \equiv \frac{\Psi + \Phi}{\Phi} = \frac{(A_6 - B_7)B_7\frac{k^2}{a^2}}{(A_6B_7 - B_6D_9)\frac{k^2}{a^2} + B_6M^2}, \tag{99}$$

$$\gamma \equiv -\frac{\Phi}{\Psi} = \frac{(A_6B_7 - B_6D_9)\frac{k^2}{a^2} + B_6M^2}{(B_7^2 - B_6D_9)\frac{k^2}{a^2} + B_6M^2}. \tag{100}$$

The aforementioned expressions for Newton's effective constant and the anisotropic stress parameters are in agreement with the ones in Ref. [80].

The subhorizon approximation is also useful as the evolution equations for the growth of matter perturbations δ_m given by Eqs. (16) and (17) can be reduced to a single differential equation, where the variable G_{eff} plays a primary role,

$$\delta_m''(a) + \left(\frac{3}{a} + \frac{H'(a)}{H(a)}\right)\delta_m'(a) - \frac{3}{2}\frac{\Omega_{m,0}G_{\mathrm{eff}}/G_N}{a^5H(a)^2/H_0^2}\delta_m(a) = 0, \tag{101}$$

with $G_{\rm eff}$ given by Eq. (97) and initial conditions $\delta_m(a_i) = a_i$ and $\delta_m'(a_i) = 1$ for an initial value for the scale factor a_i deep in the matter era.

In what follows, we will present the effective DE perturbations under the subhorizon and quasistatic approximations for two classes of models: those in which there is DE anisotropic stress and those where DE anisotropic stress vanishes.

A. Horndeski models with DE anisotropic stress

We now apply the subhorizon and quasistatic approximations in Eqs. (88)–(90) using the same prescription as in Ref. [65]. We also found, in agreement with Ref. [79], that the quasistatic approximation breaks down for this model due to the rapid oscillations of the scalar field, so if we eliminate the scalar field, then this can slightly increase the accuracy of the numerical solutions of the effective fluid equations. To eliminate $\delta\phi$ and its derivatives, we use Eq. (85) and insert the resulting equations in Eqs. (88)–(90).

Then, by keeping the dominant k^2 terms (the subhorizon approximation) and dropping time derivatives of the potentials (the quasistatic approximation) in Eqs. (88)–(90), we find

$$\frac{\delta P_{\rm DE}}{\bar\rho_{\rm DE}} \simeq \frac{1}{3\mathcal{F}_4}\frac{\frac{k^4}{a^4}\mathcal{F}_1 + \frac{k^2}{a^2}\mathcal{F}_2 + \mathcal{F}_3}{\frac{k^4}{a^4}\mathcal{F}_5 + \frac{k^2}{a^2}\mathcal{F}_6}\frac{\bar\rho_m}{\bar\rho_{\rm DE}}\delta_m, \tag{102}$$

$$\delta_{\rm DE} \simeq \frac{\frac{k^4}{a^4}\mathcal{F}_7 + \frac{k^2}{a^2}\mathcal{F}_8 + \mathcal{F}_9}{\frac{k^4}{a^4}\mathcal{F}_5 + \frac{k^2}{a^2}\mathcal{F}_6}\frac{\bar\rho_m}{\bar\rho_{\rm DE}}\delta_m, \tag{103}$$

$$V_{\rm DE} \simeq a\frac{\frac{k^2}{a^2}\mathcal{F}_{10} + \mathcal{F}_{11}}{\frac{k^2}{a^2}\mathcal{F}_5 + \mathcal{F}_6}\frac{\bar\rho_m}{\bar\rho_{\rm DE}}\delta_m, \tag{104}$$

for the effective DE pressure perturbation, effective DE density perturbation, and effective DE velocity perturbation, respectively (the interested reader can find the expressions for $\mathcal{F}_i$ in Appendix B). It is now also possible to obtain an expression for the effective DE anisotropic stress under the subhorizon approximation

$$\pi_{\rm DE} = \frac{\frac{k^2}{a^2}(\Phi+\Psi)}{\kappa\bar\rho_{\rm DE}} \simeq \frac{\frac{k^2}{a^2}\mathcal{F}_4^2 B_7(B_7 - A_6)}{\frac{k^2}{a^2}\mathcal{F}_5 + \mathcal{F}_6}\frac{\bar\rho_m}{\bar\rho_{\rm DE}}\delta_m \simeq \frac{\frac{k^4}{a^4}\mathcal{F}_4^2 B_7(B_7 - A_6)}{\frac{k^4}{a^4}\mathcal{F}_7 + \frac{k^2}{a^2}\mathcal{F}_8 + \mathcal{F}_9}\delta_{\rm DE}. \tag{105}$$

Having found expressions for the effective DE equation of state [see Eq. (73)] and the effective DE anisotropic stress [Eq. (105)], the only missing ingredient for an effective fluid description of the Horndeski Lagrangian is the sound speed. This quantity can easily be found using our equations for the effective DE pressure perturbation (102) and the effective DE density perturbation (103). The DE sound speed reads

$$c_{s,\rm DE}^2 \equiv \frac{\delta P_{\rm DE}}{\delta\rho_{\rm DE}} = \frac{1}{3}\frac{\frac{k^4}{a^4}\mathcal{F}_1 + \frac{k^2}{a^2}\mathcal{F}_2 + \mathcal{F}_3}{\frac{k^4}{a^4}\mathcal{F}_7 + \frac{k^2}{a^2}\mathcal{F}_8 + \mathcal{F}_9}. \tag{106}$$

Due to the presence of anisotropic stress, perturbations on subhorizon scales in the effective DE fluid are not driven by the sound speed (106), but by an effective DE sound speed defined as [65,82]

$$c_{s,\rm eff}^2 \equiv c_{s,\rm DE}^2 - \frac{2}{3}\pi_{\rm DE}/\delta_{\rm DE} = \frac{1}{3}\frac{\frac{k^4}{a^4}(\mathcal{F}_1 - 2\mathcal{F}_4^2 B_7(B_7 - A_6)) + \frac{k^2}{a^2}\mathcal{F}_2 + \mathcal{F}_3}{\frac{k^4}{a^4}\mathcal{F}_7 + \frac{k^2}{a^2}\mathcal{F}_8 + \mathcal{F}_9}. \tag{107}$$

Finally, it is clear that for the cosmological constant model, i.e., $\mathcal{L}_2 = -\frac{\Lambda}{\kappa}$, $\mathcal{L}_3 = 0$, $\mathcal{L}_4 = \frac{1}{2\kappa}R$, $\mathcal{L}_5 = 0$, we have $K = -\frac{\Lambda}{\kappa}$, $G_3 = 0$, $G_4 = \frac{1}{2\kappa}$, and $G_5 = 0$, which implies that $w_{\rm DE} = -1$ and $(\delta P_{\rm DE}, \delta\rho_{\rm DE}, \pi_{\rm DE}) = (0,0,0)$ as expected.

1. *f(R)* models

Thus far we have kept the discussion quite general; that is to say, we did not specify any function in the Horndeski Lagrangian (21). To mention an example, we will present the results for $f(R)$ models. With the definitions in Eqs. (25) and (26) and using units where $\kappa = 1$, one obtains

$$\begin{aligned}
&B_7 = 2A_6 = 2, \qquad B_6 = B_8 = 2\phi, \qquad D_9 = 0,\\
&\mathcal{F}_1 = \mathcal{F}_4 = -1/2, \qquad \mathcal{F}_2 = -\frac{15\ddot F}{4}, \qquad \mathcal{F}_3 = -\frac{2F\ddot F}{4F_{,R}},\\
&\mathcal{F}_5 = -\frac{3F}{2}, \qquad \mathcal{F}_6 = -\frac{F^2}{2F_{,R}}, \qquad \mathcal{F}_7 = -1 + \frac{3F}{2},\\
&\mathcal{F}_8 = \frac{(F-1)F}{2F_{,R}}, \qquad \mathcal{F}_9 = 0, \qquad \mathcal{F}_{10} = -\frac{3\dot F}{2},\\
&\mathcal{F}_{11} = -\frac{F\dot F}{4F_{,R}}, \qquad M^2 = -K_{\phi\phi} = \frac{1}{2f_{RR}},
\end{aligned} \tag{108}$$

where

$$K_\phi = \frac{dK}{d\phi} = \frac{dK}{dR}\frac{dR}{d\phi} = \frac{1}{2f_{,RR}}(Rf_{,RR}) = -\frac{R}{2}, \tag{109}$$

$$K_{\phi\phi} = \frac{d}{d\phi}\left(\frac{dK}{d\phi} = -\frac{R}{2}\right) = \frac{1}{f_{,RR}}\frac{d}{dR}\left(-\frac{R}{2}\right) = -\frac{1}{2f_{RR}}, \tag{110}$$

and $F = f_{,R}$, $F_{,R} = f_{,RR}$. Then, the effective DE fluid quantities read

$$\frac{\delta P_{\rm DE}}{\bar\rho_{\rm DE}} \simeq \frac{1}{3F}\frac{2\frac{k^2}{a^2}\frac{F_{,R}}{F} + 3(1+5\frac{k^2}{a^2}\frac{F_{,R}}{F})\ddot F k^{-2}}{1+3\frac{k^2}{a^2}\frac{F_{,R}}{F}}\frac{\bar\rho_m}{\bar\rho_{\rm DE}}\delta_m, \tag{111}$$

$$\delta_{\rm DE} \simeq \frac{1}{F}\frac{1-F+\frac{k^2}{a^2}(2-3F)\frac{F_{,R}}{F}}{1+3\frac{k^2}{a^2}\frac{F_{,R}}{F}}\frac{\bar\rho_m}{\bar\rho_{\rm DE}}\delta_m, \tag{112}$$

$$V_{\rm DE} \simeq \frac{a\dot F}{2F}\frac{1+6\frac{k^2}{a^2}\frac{F_{,R}}{F}}{1+3\frac{k^2}{a^2}\frac{F_{,R}}{F}}\frac{\bar\rho_m}{\bar\rho_{\rm DE}}\delta_m. \tag{113}$$

$$\pi_{\rm DE} \simeq \frac{1}{F}\frac{\frac{k^2}{a^2}\frac{F_{,R}}{F}}{1+3\frac{k^2}{a^2}\frac{F_{,R}}{F}}\frac{\bar\rho_m}{\bar\rho_{\rm DE}}\delta_m \simeq \frac{\frac{k^2}{a^2}\frac{F_{,R}}{F}}{1-F+\frac{k^2}{a^2}(2-3F)\frac{F_{,R}}{F}}\delta_{\rm DE}. \tag{114}$$

$$c^2_{s,\rm DE} \simeq \frac{1}{3}\frac{2\frac{k^2}{a^2}\frac{F_{,R}}{F} + 3(1+5\frac{k^2}{a^2}\frac{F_{,R}}{F})\ddot F k^{-2}}{1-F+\frac{k^2}{a^2}(2-3F)\frac{F_{,R}}{F}}, \tag{115}$$

$$c^2_{s,\rm eff} \simeq \frac{(1+5\frac{k^2}{a^2}\frac{F_{,R}}{F})\ddot F k^{-2}}{1-F+\frac{k^2}{a^2}(2-3F)\frac{F_{,R}}{F}}. \tag{116}$$

These results are in perfect agreement with our previous work [65].

B. Horndeski models with no dark energy anisotropic stress

With the same approach that we followed in Sec. IV A we compute the DE perturbations for models where there is no DE anisotropic stress, i.e., $\Phi = -\Psi$. With this restriction it is easy to see from Eq. (85) that $G_{4\phi} = 0$. Then applying this condition under the subhorizon approximation in Eqs. (88)–(90) leads to

$$\frac{\delta P_{\rm DE}}{\bar\rho_{\rm DE}} \simeq \frac{1}{3}\frac{\frac{k^2}{a^2}\hat{\mathcal F}_2 + \hat{\mathcal F}_3}{\frac{k^4}{a^4}\hat{\mathcal F}_5 + \frac{k^2}{a^2}\hat{\mathcal F}_6}\frac{\bar\rho_m}{\bar\rho_{\rm DE}}\delta_m, \tag{117}$$

$$\delta_{\rm DE} \simeq \frac{\frac{k^4}{a^4}\hat{\mathcal F}_7 + \frac{k^2}{a^2}\hat{\mathcal F}_8 + \hat{\mathcal F}_9}{\frac{k^4}{a^4}\hat{\mathcal F}_5 + \frac{k^2}{a^2}\hat{\mathcal F}_6}\frac{\bar\rho_m}{\bar\rho_{\rm DE}}\delta_m, \tag{118}$$

$$V_{\rm DE} \simeq a\frac{\frac{k^2}{a^2}\hat{\mathcal F}_{10} + \hat{\mathcal F}_{11}}{\frac{k^2}{a^2}\hat{\mathcal F}_5 + \hat{\mathcal F}_6}\frac{\bar\rho_m}{\bar\rho_{\rm DE}}\delta_m, \tag{119}$$

and since $\Phi = -\Psi$, the anisotropic parameters read

$$\eta \equiv \frac{\Psi+\Phi}{\Phi} = 0, \tag{120}$$

$$\gamma \equiv -\frac{\Phi}{\Psi} = 1, \tag{121}$$

as expected, while the DE anisotropic stress parameter is zero $\pi_{\rm DE} = 0$. Our general expression for the DE sound speed (106) reduces in this case to

$$c^2_{s,\rm DE} = \frac{\frac{k^2}{a^2}\hat{\mathcal F}_2 + \hat{\mathcal F}_3}{\frac{k^4}{a^4}\hat{\mathcal F}_7 + \frac{k^2}{a^2}\hat{\mathcal F}_8 + \hat{\mathcal F}_9}, \tag{122}$$

which is equal to the DE effective sound speed since $\pi_{\rm DE} = 0$. Here we will show results for a few specific models embedded in the Horndeski Lagrangian.

1. Quintessence

We can recover the Lagrangian of quintessence by choosing the following functions:

$$K = X - V(\phi), \qquad G_4 = \frac{1}{2\kappa}, \tag{123}$$

where ϕ is the scalar field, X is the kinetic term defined as $X = -\frac{1}{2}g^{\mu\nu}\partial_\mu\phi\partial_\nu\phi$, and $V(\phi)$ is the potential. Using a variational approach one finds that the effective pressure, density, and velocity perturbations for quintessence theories are given by

$$\delta P_{\rm DE} = (\dot\phi\,\delta\dot\phi - \Psi\dot\phi^2) - V_\phi\delta\phi,$$
$$\rho_{\rm DE}\delta_{\rm DE} = (\dot\phi\,\delta\dot\phi - \Psi\dot\phi^2) + V_\phi\delta\phi, \tag{124}$$

$$V_{\rm DE} = \frac{k^2}{a}\dot\phi\delta\phi, \tag{125}$$

and these expressions are in agreement with [83]. Also, the DE anisotropic stress parameter $\pi_{\rm DE}$ is zero since for quintessence $\Psi = -\Phi$. We find that under the subhorizon approximation

$$A_6 = 0, \quad B_6 = -2, \quad D_9 = -K_X, \quad M^2 = -K_{\phi\phi}, \tag{126}$$

so that the effective pressure, density, and velocity perturbations for quintessence theories are given by

$$\frac{\delta P_{\rm DE}}{\bar\rho_{\rm DE}} \simeq \frac{\dot\phi^2}{2k^2/a^2}\frac{\bar\rho_m}{\bar\rho_{\rm DE}}\delta_m, \tag{127}$$

$$\delta_{\rm DE} \simeq \frac{\dot\phi^2}{2k^2/a^2}\frac{\bar\rho_m}{\bar\rho_{\rm DE}}\delta_m, \tag{128}$$

$$V_{\rm DE} \simeq 0. \tag{129}$$

It is thus straightforward, using Eqs. (127) and (128), to see that the DE sound speed is given by

$$c^2_{s,\rm DE} = 1. \tag{130}$$

Moreover, we also find that in the subhorizon approximation

$$\delta\phi \simeq 0,$$
$$\Psi \simeq -\frac{\bar\rho_m\delta_m a^2}{2k^2}. \tag{131}$$

2. K-essence

In our notation the Lagrangian of K-essence theories is specified by the functions [84,85]

$$K(\phi, X) = P(\phi, X), \qquad G_4 = \frac{1}{2\kappa}, \tag{132}$$

and as usual through the variation of the action it is possible to find expressions for the pressure, density, and velocity perturbations

$$\delta P_{\rm DE} = P_\phi\delta\phi + P_X(\dot\phi\,\delta\dot\phi - \dot\phi^2\Psi), \tag{133}$$

$$\rho_{\rm DE}\delta_{\rm DE} = \delta\phi(P_{X\phi}\dot\phi^2 - P_\phi) - \dot\phi(P_X + P_{XX}\dot\phi^2)(\dot\phi\Psi - \delta\dot\phi), \tag{134}$$

$$V_{\rm DE} = \frac{k^2}{a}P_X\dot\phi\delta\phi. \tag{135}$$

Since for K-essence $\Psi = -\Phi$, the DE anisotropic stress parameter $\pi_{\rm DE}$ vanishes. We find that under the subhorizon approximation

$$A_6 = 0, \qquad B_6 = -2, \qquad D_9 = -P_X, \qquad M^2 = -P_{\phi\phi}, \tag{136}$$

and therefore the DE perturbations for K-essence theories are given by

$$\frac{\delta P_{\rm DE}}{\bar\rho_{\rm DE}} \simeq \frac{P_X\dot\phi^2}{2k^2/a^2}\frac{\bar\rho_m}{\bar\rho_{\rm DE}}\delta_m, \tag{137}$$

$$\delta_{\rm DE} \simeq \frac{\dot\phi^2(P_X + P_{XX}\dot\phi^2)}{2k^2/a^2}\frac{\bar\rho_m}{\bar\rho_{\rm DE}}\delta_m, \tag{138}$$

$$V_{\rm DE} \simeq 0, \tag{139}$$

and the DE sound speed reads

$$c^2_{s,\rm DE} = \frac{P_X}{P_X + 2XP_{XX}}, \tag{140}$$

in agreement with Refs. [84,85]. The perturbations of the scalar field and the gravitational potential are, respectively, given by

$$\delta\phi \simeq 0,$$
$$\Psi \simeq -\frac{\bar\rho_m\delta_m a^2}{2k^2}. \tag{141}$$

3. Kinetic gravity braiding

An interesting DE model is the kinetic gravity braiding (KGB) which is characterized by the following Lagrangian:

$$K = K(X), \qquad G_3 = G_3(X), \qquad G_4 = \frac{1}{2\kappa}. \tag{142}$$

Since G_4 is constant, it is easily shown from Eq. (92) that the KGB model has no DE anisotropic stress and therefore the anisotropic parameters

$$\eta \equiv \frac{\Psi + \Phi}{\Phi} = 0, \tag{143}$$

$$\gamma \equiv -\frac{\Phi}{\Psi} = 1. \tag{144}$$

Furthermore, it follows that the effective Newton's constant $G_{\rm eff}/G_N$ is given by

$$G_{\rm eff}/G_N = \frac{M^2 - D_9\frac{k^2}{a^2}}{M^2 - (D_9 + A_6^2/2)\frac{k^2}{a^2}}. \tag{145}$$

The effective DE density and pressure $\bar\rho_{\rm DE}$ and $\bar P_{\rm DE}$ read, respectively,

$$\kappa\bar\rho_{\rm DE} = -K + \dot\phi^2(-G_{3\phi} + K_X + 3G_{3X}H\dot\phi), \tag{146}$$

$$\kappa\bar P_{\rm DE} = K - \dot\phi^2(G_{3\phi} + G_{3X}\ddot\phi), \tag{147}$$

and therefore the DE equation of state is given by

$$w_{\rm DE} = \frac{K - \dot\phi^2(G_{3\phi} + G_{3X}\ddot\phi)}{-K + \dot\phi^2(-G_{3\phi} + K_X + 3G_{3X}H\dot\phi)}. \tag{148}$$

We also find that the scalar field equation at the background level is

$$K_\phi - (K_X - 2G_{3\phi})(\ddot{\phi} + 3H\dot{\phi}) - K_{X\phi}\dot{\phi}^2 - K_{XX}\ddot{\phi}\dot{\phi}^2 + G_{3\phi\phi}\dot{\phi}^2 + G_{3X\phi}\dot{\phi}^2(\ddot{\phi} - 3H\dot{\phi}) - 3G_{3X}(2H\ddot{\phi}\dot{\phi} + 3H^2\dot{\phi}^2 + \dot{H}\dot{\phi}^2) - 3G_{3XX}H\ddot{\phi}\dot{\phi}^3 = 0. \tag{149}$$

As a specific example we now discuss the KGB model of Ref. [79] defined by

$$K(X) = -X, \tag{150}$$

$$G_3(X) = \frac{1}{\sqrt{\kappa}}(\kappa r_c^2 X)^n = \alpha X^n, \tag{151}$$

where n and α are parameters in the model. A number of reasons make the KGB an attractive model. First, it passes the recent observational constraints from gravitational waves. Second, it is known that this model connects the original Galileon model [64] and the ΛCDM model by the parameter n, at least for the background and first order perturbations: linear perturbations of the KGB model reduce to those of ΛCDM (original Galileon) for $n = \infty$ ($n = 1$) [79].

The charge density of the Noether current Eq. (79) is in this case

$$J_0 = \dot{\phi}(3\dot{\phi}G_{3X}H - 1) \tag{152}$$

and satisfies the differential equation

$$\dot{J}_0 + 3HJ_0 = 0, \tag{153}$$

whose solution reads

$$J_0 = \frac{J_c}{a^3} \tag{154}$$

with J_c a constant. It is therefore clear that J_0 approaches zero as the Universe expands. The simplest attractor solution is located at $J_0 = 0$ and has two branches, namely,

$$\dot{\phi} = 0 \tag{155}$$

and

$$\dot{\phi} = \frac{1}{3G_{3X}H}. \tag{156}$$

Because the first case has ghostly perturbations, as it is shown in [79], we will focus on the attractor solution Eq. (156). Using Eqs. (71) and (152) we find that the modified Friedmann equation is given by

$$\left(\frac{H}{H_0}\right)^2 = (1 - \Omega_{m,0})\left(\frac{H}{H_0}\right)^{-\frac{2}{2n-1}} + \Omega_{m,0}a^{-3}, \tag{157}$$

where we have neglected radiation. The background equation of the KGB model reduces to that of ΛCDM for $n = \infty$ as can be seen from Eq. (157). Also, one can easily find an expression for the parameter α by using Eq. (157) at the present epoch

$$\alpha = \left(\frac{2^{n-1}}{3n}\right)\left(\frac{1}{6(1 - \Omega_{m,0})}\right)^{\frac{2n-1}{2}}. \tag{158}$$

The DE equation of state becomes

$$w_{\rm DE} = \frac{\bar{P}_{\rm DE}}{\bar{\rho}_{\rm DE}} = \frac{2\dot{H}}{3(2n-1)} - 1, \tag{159}$$

and through Eq. (156) it is also possible to find an analytical expression for the kinetic term

$$X = \frac{1}{2}a^2H^2\phi'(a)^2 = 3H_0^2(1 - \Omega_{m,0})\left(\frac{H}{H_0}\right)^{\frac{2n}{1-2n}}, \tag{160}$$

where the prime stands for the derivative with respect to the scale factor.

To derive the ΛCDM limit for the perturbations in this model we rewrite Eqs. (84) and (86) in terms of the kinetic term perturbation $\delta X = \dot{\phi}\,\delta\dot{\phi} - \dot{\phi}^2\Psi$. Then, for $n \to \infty$ the former equation reduces to $\delta X(-\frac{2}{a} - \frac{H'(a)}{H(a)} + O(1/n))$, while the latter equation gives

$$\delta\dot{X} + 3H\delta X = 0, \tag{161}$$

which implies that the kinetic term perturbation decays as $\delta X \sim 1/a^3$ and thus can be ignored at late time. Since DE perturbations in the KGB model are proportional to δX for large n, then they reduce to zero as expected for the ΛCDM model.

Finally, it should be noted that a standard hydrodynamical description of the KGB in terms of an effective fluid has been studied in Ref. [86]. There, it was shown that the KGB model can also be described in terms of an imperfect fluid with a chemical potential, in which the equations of motion reduce to the standard diffusion equation. However, in our current analysis we will only focus on the ideal fluid approach, which is totally equivalent, as we are interested in finding simple analytic solutions and with comparing with our previous work.

V. DESIGNER HORNDESKI

In this section we will address the shortcomings found in the KGB model defined by Eqs. (150) and (151). We will show that it is possible, starting from the Lagrangian (142), to find a model corresponding to a given background but yet having different perturbations. Using the modified Friedmann equation and the scalar field conservation equation, we can find specific designer models such that

the background is always that of the ΛCDM model, namely, having $w_{\rm DE} = -1$. This is particularly useful in detecting deviations from ΛCDM at the perturbations level and is a natural expansion of our earlier work [40,65]. We start with the modified Friedmann equation, which can be written as

$$-H(a)^2 - \frac{K(X)}{3} + H_0^2\Omega_m(a) + 2\sqrt{2}X^{3/2}H(a)G_{3X} + \frac{2}{3}XK_X = 0, \tag{162}$$

while the scalar field conservation equation can be written as

$$\frac{J_c}{a^3} - 6XH(a)G_{3X} - \sqrt{2}\sqrt{X}K_X = 0, \tag{163}$$

where J_c is a constant which quantifies our deviation from the attractor, as in the case of the KGB model [79]. We now have two equations given by (162) and (163), but three unknown functions $(G_{3X}(X), K(X), H(a))$, and thus the system is undetermined. Therefore, we need to specify one of the three unknown functions $(G_{3X}(X), K(X), H(a))$ and determine the other two using Eqs. (162) and (163). To facilitate this, we express the Hubble parameter as a function of the kinetic term X, i.e., $H = H(X)$ and then solve the previous equations to find $(G_{3X}(X), K(X))$. Doing so yields

$$K(X) = -3H_0^2\Omega_{\Lambda,0} + \frac{J_c\sqrt{2X}H(X)^2}{H_0^2\Omega_{m,0}} - \frac{J_c\sqrt{2X}\Omega_{\Lambda,0}}{\Omega_{m,0}},$$
$$G_{3X}(X) = -\frac{2J_cH'(X)}{3H_0^2\Omega_{m,0}}. \tag{164}$$

With Eqs. (164) we can make a whole family of designer models that behave as ΛCDM at the background level but have different perturbations. We now proceed to specify some examples using our formalism.

A. Example 1

Choosing $K(X) = 0$ and solving Eqs. (164) we find

$$K(X) = 0,$$
$$G_3(X) = -\frac{\sqrt{2J_c}\sqrt{\Omega_{\Lambda,0}(2J_c\sqrt{X} + 3\sqrt{2}H_0^2\Omega_{m,0})}}{3H_0X^{1/4}\Omega_{m,0}}, \tag{165}$$

and the derivative of the scalar field $\phi'(a)$ is

$$\phi'(a) = \frac{3a^2H_0^2\Omega_{\Lambda,0}}{J_cH(a)}, \tag{166}$$

where the prime is the derivative with respect to the scale factor. However, this model has the problem that it does not have a smooth limit to ΛCDM when $J_c = 0$.

B. Example 2

On the other hand, specifying $G_3(X)$ leads to another interesting designer model, defined as

$$G_3(X) = G_{30}X,$$
$$K(X) = -3H_0^2\Omega_{\Lambda,0} + \frac{9H_0^2(X - X_0)^2G_{30}^2\sqrt{X}\Omega_{m,0}}{2\sqrt{2}J_c} - \frac{\sqrt{2}J_c\sqrt{X}\Omega_{\Lambda,0}}{\Omega_{m,0}}, \tag{167}$$

where the kinetic term is defined as

$$X = \frac{3G_{30}H_0X_0\Omega_{m,0} - 2J_cH(a)}{3G_{30}H_0^2\Omega_{m,0}} \tag{168}$$

and X_0 is an integration constant. However, this model has the problem that at early times the perturbations do not go to zero and we do not recover GR, since the kinetic term goes to infinity as it grows as $X \sim H(a)$.

C. Example 3 (HDES)

To solve the previous shortcomings we follow a different approach. First, we demand that the kinetic term behaves as $X = \frac{c_0}{H(a)^n}$, where $c_0 > 0$ and $n > 0$. Then, from Eqs. (163) and (162) we find

$$G_3(X) = -\frac{2J_cc_0^{1/n}X^{-1/n}}{3H_0^2\Omega_{m,0}},$$
$$K(X) = \frac{\sqrt{2}J_cc_0^{2/n}X^{\frac{1}{2}-\frac{2}{n}}}{H_0^2\Omega_{m,0}} - 3H_0^2\Omega_{\Lambda,0} - \frac{\sqrt{2}J_c\sqrt{X}\Omega_{\Lambda,0}}{\Omega_{m,0}}. \tag{169}$$

This specific model solves both previous problems, i.e., it has a smooth limit to ΛCDM, and it also recovers GR when $J_c \sim 0$; thus we will designate this model as HDES and focus on it in what follows.

D. Comparison with the α parameters

To facilitate comparisons with the literature we also provide the expressions for our designer HDES model in terms of the α_i functions, where $i = M, K, B, T$. The functions $G_i(\phi, X)$ and α_i are connected in the following manner [70]:

$$
\begin{aligned}
M_*^2 &\equiv 2(G_4 - 2XG_{4X} - \dot{\phi}HXG_{5X} + XG_{5\phi}),\\
\alpha_M &\equiv \frac{d\ln M_*^2}{d\ln a},\\
H^2M_*^2\alpha_K &\equiv 2X(G_{2X} + 2XG_{2XX} - 2G_{3\phi} - 2XG_{3\phi X})\\
&\quad + 12H\dot{\phi}X[G_{3X} + XG_{3XX} - 3G_{4\phi X}\\
&\quad - 2XG_{4\phi XX}]\\
&\quad + 12H^2X[G_{4X} - G_{5\phi} + X(8G_{4XX} - 5G_{5\phi X})\\
&\quad + 2X^2(2G_{4XXX} - G_{5\phi XX})]\\
&\quad + 4H^3\dot{\phi}X(3G_{5X} + 7XG_{5XX} + 2X^2G_{5XXX}),\\
H^2M_*^2\alpha_B &\equiv 2\dot{\phi}(XG_{3X} - G_{4\phi} - 2XG_{4\phi X})\\
&\quad + 8HX(G_{4X} + 2XG_{4XX} - G_{5\phi} - XG_{5\phi X})\\
&\quad + \frac{2H^2\phi' X}{a}(3G_{5X} + 2XG_{5XX}),\\
M_*^2\alpha_T &\equiv 4X(G_{4X} - G_{5\phi}) - 2X(\ddot{\phi} - 2H\dot{\phi})G_{5X},
\end{aligned}
\tag{170}
$$

where the dot is the derivative with respect to the cosmic time, $M_*^2(\tau)$ is the cosmological strength of gravity, α_T is the tensor speed excess, α_B is called the braiding, and α_K is referred to as the kineticity. For more information on these α_i functions see [87]. At all times we require $D = \alpha_K + \frac{3}{2}\alpha_B^2 > 0$ so that there are no ghostly instabilities and that $\alpha_{M,K,B,T} \simeq 0$ at early times, so as to recover GR.

For our HDES designer model given by Eqs. (169), we have that the α_i functions of Eq. (170) are given by

$$M_*^2 \equiv 1, \tag{171}$$

$$\alpha_M \equiv \frac{d\ln M_*^2}{d\ln a} = 0, \tag{172}$$

$$\alpha_K \equiv -\frac{4\sqrt{2}\sqrt{c_0}J_c(n-2)H(a)^{-\frac{n}{2}}}{H_0^2n^2\Omega_{m,0}}, \tag{173}$$

$$\alpha_B \equiv \frac{4\sqrt{2}\sqrt{c_0}J_cH(a)^{-\frac{n}{2}}}{3H_0^2n\Omega_{m,0}}, \tag{174}$$

$$\alpha_T \equiv 0. \tag{175}$$

Since in Eqs. (173) and (174) we have a degeneracy with the coefficients c_0 and J_c—they appear together as $\sqrt{c_0}J_c$—we can choose to absorb c_0 in the definition of J_c. Finally, it is straightforward to see that our α_i functions are dimensionless since through dimensional analysis we found that $[c_0] = H_0^{n+2}$, $[J_c] = H_0$, the kinetic term $[X] = H_0^2$, $[K] = H_0^2$, and $[G_{3X}] = H_0^{-2}$.

Notice that not all designer models satisfy the above conditions, so in what follows we consider only HDES, given by Eq. (169). Then, the stability condition $D = \alpha_K + \frac{3}{2}\alpha_B^2 > 0$ for our model Eq. (169) gives

$$\tilde{J}_c\left(4\tilde{J}_c - 3\sqrt{2}(n-2)\Omega_{m,0}\left(\frac{H(a)}{H_0}\right)^{n/2}\right) > 0, \tag{176}$$

where we have set $\tilde{J}_c = J_c/H_0$ and $\tilde{c}_0 = c_0/H_0^{n+2} = 1$.

Then, inequality (176) implies that in order for the system to be stable we must have either $\tilde{J}_c > 0$ for $0 < n \leq 2$ or a complicated set of expressions that can, however, be easily derived from Eq. (176) with algebraic manipulations. For $n = 2$ the inequality is automatically satisfied for any value of $\tilde{J}_c$ as $\alpha_K = 0$ as can be seen from Eq. (173). We show the complicated parameter space that is allowed for $n = 1$ and $n = 3$ as a function of scale factor a but also as a function of n for $a = 1$, in Fig. 1.

E. Analytic solutions for the growth

Furthermore, in this case we can also find approximate solutions to the growth equation Eq. (101) in matter domination for $n = 2$. To do this, we first do a series expansion around $a = 0$ to the $G_{\rm eff}$ of Eq. (97), which gives

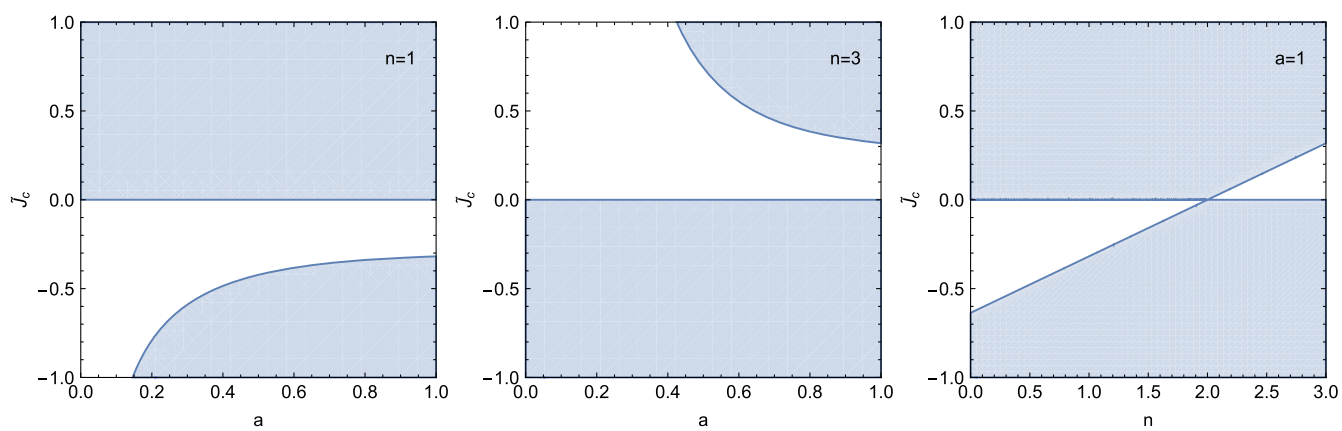

FIG. 1. The allowed parameter space (shaded region) so that $D > 0$ for $n = 1$ (left) and $n = 3$ (center) and $a = 1$ for $\Omega_{m,0} = 0.3$. In the case of $n = 2$, all values of $\tilde{J}_c$ are allowed.

$$G_{\rm eff}/G_N = 1 + \frac{\sqrt{2}\tilde{J}_c}{3\Omega_{m,0}H(a)/H_0}, \tag{177}$$

which we can use to solve Eq. (101) in matter domination, where $H(a)/H_0 \simeq \sqrt{\Omega_{m,0}a^{-3}}$. Then, we get

$$\delta_m(a) = \frac{3^{5/3}\Omega_{m,0}^{5/4}\Gamma(\frac{8}{3})}{2^{5/4}\tilde{J}_c^{5/6}} a^{-1/4} I_{\frac{5}{3}}\left(\frac{2^{7/4}\sqrt{\tilde{J}_c}}{3\Omega_{m,0}^{3/4}} a^{3/4}\right), \tag{178}$$

where $I_n(z)$ is the modified Bessel function of the first kind and $\Gamma(n)$ is the usual Gamma function. Using Eq. (178) and the definition of the growth rate $f\sigma_8(a) \equiv f(a)\cdot\sigma(a) = \sigma_8 a\delta_m'(a)/\delta_m(a=1)$, we can calculate the latter exactly. However, it is instructive to perform a series expansion around $a = 1$, which gives

$$f\sigma_8(a) \simeq \sigma_8\left(\frac{1}{2}\left(\frac{5\alpha_1}{\alpha_2} - 3\right) + \frac{1}{4}\left(-\frac{5\alpha_1}{\alpha_2} + \frac{2\sqrt{2}\tilde{J}_c}{\Omega_{m,0}^{3/2}} + 9\right)(a-1) + \cdots\right), \tag{179}$$

where we have defined the parameters

$$\alpha_1 = {}_0F_1\left(\frac{5}{3}; \frac{2\sqrt{2}\tilde{J}_c}{9\Omega_{m,0}^{3/2}}\right), \tag{180}$$

$$\alpha_2 = {}_0F_1\left(\frac{8}{3}; \frac{2\sqrt{2}\tilde{J}_c}{9\Omega_{m,0}^{3/2}}\right), \tag{181}$$

where ${}_0F_1(c_1, z)$ is a hypergeometric function.

As can be seen from Eq. (179) there is a strong degeneracy between $\tilde{J}_c$ and σ_8, which can also be demonstrated by doing a series expansion of $f\sigma_8(a=1)$ for small $\tilde{J}_c$, which gives

$$f\sigma_8(a=1) \simeq \sigma_8\left(1 + \frac{\tilde{J}_c}{4\sqrt{2}\Omega_{m,0}^{3/2}} + \cdots\right), \tag{182}$$

which implies that if we keep the growth today given constant, i.e., $f\sigma_8(a=1) = C_0 = \text{const}$, then σ_8 will scale roughly as

$$\sigma_8 \simeq C_0\left(1 - \frac{\tilde{J}_c}{4\sqrt{2}\Omega_{m,0}^{3/2}} + \cdots\right). \tag{183}$$

Since $\Omega_{m,0}$ is strongly constrained from Planck, we expect that the low redshift $f\sigma_8$ data will exhibit a degeneracy between $\tilde{J}_c$ and σ_8. More specifically, by inspecting Eq. (183) we expect a strong negative correlation between the two parameters, and this is exactly what we see from the actual Markov Chain–Monte Carlo (MCMCs) that we present in later sections. This degeneracy is interesting as it can potentially alleviate the soft 2σ tension between the growth rate data ($\sigma_8 = 0.88$) and Planck ($\sigma_8 = 0.831$), which has been extensively discussed in the literature; see Refs. [27,88] and references therein.

VI. NUMERICAL SOLUTIONS

Here we present the numerical solutions of the two models, the KGB and HDES, that we described in the previous section.

A. The KGB model

1. The attractor

To explore the possibility of working outside the attractor we only need to use Eqs. (71) and (152), as these constrain J_c and α with $H(a=1) = H_0$. To parametrize the deviation from the attractor we will use the parameter J_c. An illustrative example is found in Fig. 2 where we plot the dark energy density $\Omega_{\rm DE}$ with respect to the scale factor for several values of n (left) and J_c (right). The values of values for J_c were chosen so as to highlight the differences of these models with respect to GR.

In the KGB model the DE density can be written via Eq. (69) as

$$\Omega_{\rm DE} = \frac{\rho_{\rm DE}}{\rho_c}, \tag{184}$$

$$\rho_{\rm DE} = -K + K_X\dot{\phi}^2 - G_{3\phi}\dot{\phi}^2 + 3G_{3X}H\dot{\phi}^3. \tag{185}$$

From Fig. 2 we can see that working outside the attractor for the KGB model ($n = 1$) we might find new parts of the parameter space and new phenomenology. In the right panel of Fig. 2, we see that the orange line can be ruled out because it predicts a very high value for the DE density at early times. The red and green lines, although outside the attractor solution, are plausible solutions that are interesting to analyze in more depth.

2. Numerical solution

In this section we present the results of the numerical solution of the evolution equations. In all cases we will assume $\Omega_{m,0} = 0.3$, $k = 300H_0$, and $\sigma_{8,0} = 0.8$, unless otherwise specified. The reason we choose the specific value of $k = 300H_0 \sim 0.1h/\text{Mpc}$ for the wave number is that it corresponds to the largest value of k we can choose without entering the nonlinear regime. Finally, we set the initial conditions for the DE variables to zero at $a_i = 10^{-3}$, when we are well inside the matter dominated regime.

Next we will also present our results for the growth rate of matter perturbations parameter $f\sigma_8(a) \equiv f(a)\cdot\sigma(a)$,

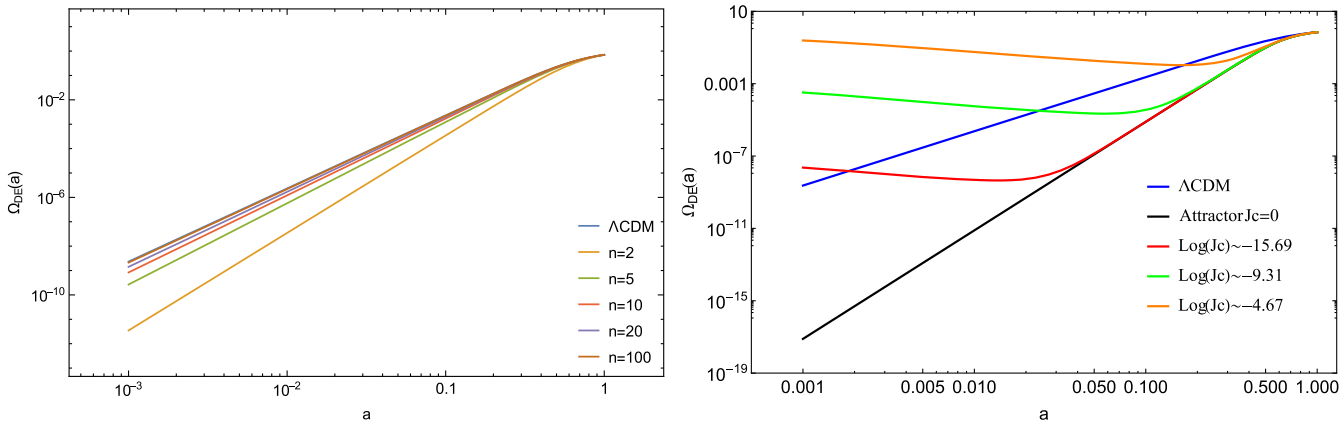

FIG. 2. The DE density for the KGB model for various values of n (left) and for the KGB model ($n = 1$) for the attractor and three general cases outside the attractor given by different values of J_c, chosen so as to highlight the differences of these models with respect to GR. The left panel clearly shows that as n grows, the DE density approaches that of the ΛCDM model.

where $f(a) = \frac{dln\delta}{dlna}$ is the growth rate and $\sigma(a) = \sigma_{8,0}\frac{\delta(a)}{\delta(1)}$ is the redshift-dependent rms fluctuations of the linear density field within spheres of radius $R = 8h^{-1}$ Mpc, while the parameter $\sigma_{8,0}$ is its value today. The $f\sigma_8(a)$ parameter is important as it can be shown to be not only independent of the bias b_1 but also a good discriminator of DE models. The reason for this is that in linear theory the quadrupole contribution to the galaxy power spectrum in redshift space is sensitive only to the combination $f\sigma_8(a)$.

Specifically, here we will compare the numerical solutions for the following cases:

(i) The numerical solution of the full system of equations given by Eqs. (82)–(85), which, however, we rewrite in terms of $\delta X = \dot{\phi}\,\dot{\delta\phi} - \dot{\phi}^2\Psi$ as the system is more stable this way. We call this case "full KGB."

(ii) The numerical solution of the effective fluid approach given by Eqs. (16) and (17). We call this case "eff. fluid."

(iii) The numerical solution of the growth factor equation (101). We call this case "ODE-Geff."

(iv) The ΛCDM model.

In the left panel of Fig. 3 we show the evolution of the matter and effective DE perturbation variables $(\delta_m, V_m, \delta_{DE}, V_{DE})$ for the KGB for $n = 2$. In the right panel we show the evolution of the $f\sigma_8(z)$ parameter for the KGB model for $n = 2$ and $\sigma_{8,0} = 0.8$ versus the $f\sigma_8$ data compilation from Ref. [88]. We show the theoretical curves for the full KGB brute-force solution, the effective fluid approach, the ΛCDM model, and the numerical solution of the G_{eff} equation. As can be seen, the agreement with all approaches is excellent.

An interesting thing to note in Fig. 3 is that $V_{DE} > \delta_{DE}$ and $V_{DE} \sim V_m$ at intermediate redshift. The reason for this is that in the effective fluid approach the DE velocity perturbations are not always subdominant, as it would be expected in a general DE fluid. This can be seen by remembering that the velocity perturbations are

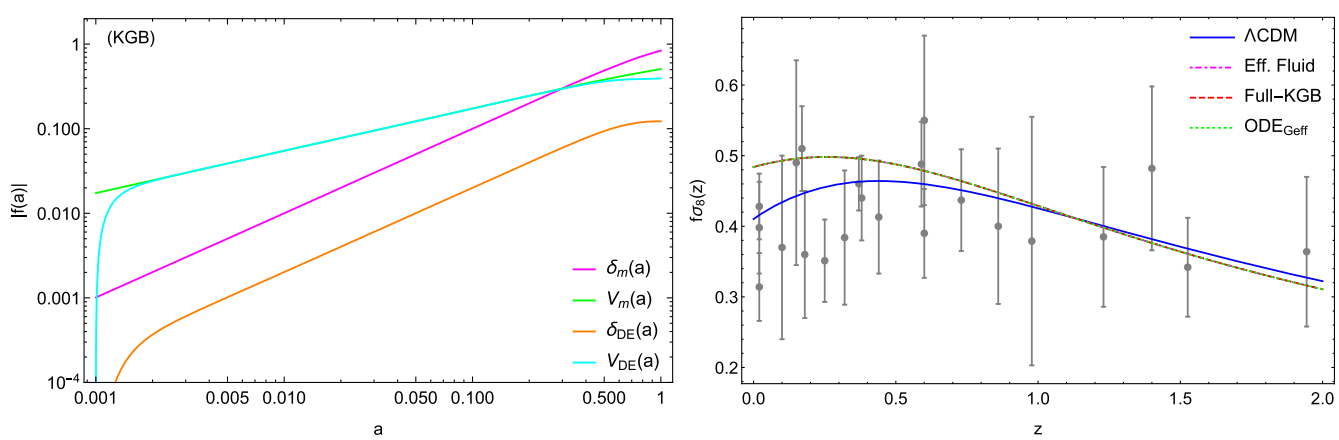

FIG. 3. Left: The evolution of the matter and effective DE perturbation variables $(\delta_m, V_m, \delta_{DE}, V_{DE})$ for the KGB with $n = 2$. Right: The evolution of the $f\sigma_8(z)$ parameter for the KGB model with $n = 2$ and $\sigma_{8,0} = 0.8$ versus the $f\sigma_8$ data compilation from Ref. [88]. Here we show the theoretical curves for the "full KGB" brute-force solution, the effective fluid approach, the ΛCDM model, and the numerical solution of the G_{eff} equation. As can be seen, the agreement with all approaches is excellent.

actually a component of the effective energy momentum tensor, namely the T_i^0 part, and thus they contain some of the main contributions of the modified gravity theory and can be in some cases rather large. See, for example, Eqs. (6) and (17) for the definition of $V_{\rm DE}$ and Eqs. (83) and (90) for all of the extra terms that are rewritten as $V_{\rm DE}$.

As an example, also consider the case of quintessence and k essense, where $V_{\rm DE}$ is proportional to the scalar field perturbations; see Eqs. (125) and (135), respectively. In the case of $f(R)$, $V_{\rm DE}$ is given by (113) and is proportional to $\dot{F}/F$, which parametrizes the deviations from GR, so it is a proxy for the $f(R)$ modified gravity perturbations.

However, in the case of the KGB model the subhorizon approximation fails when the parameter n is large. This can easily be seen by calculating the large n limit of the $G_{\rm eff}$ parameter via Eq. (97):

$$G_{\rm eff}/G_N \simeq 1 + \frac{2a^3(1-\Omega_{m,0})}{5\Omega_{m,0}}, \tag{186}$$

which at $a = 1$ tends to $G_{\rm eff}/G_N \simeq \frac{3}{5} + \frac{2}{5\Omega_{m,0}}$, which is different from unity as expected at this limit. However, in general deviations of $G_{\rm eff}/G_N$ from unity on such scales are not problematic as screening mechanisms play an important role. In any case, our finding is in agreement with what was previously found in Ref. [79]; namely, the quasistatic approximation breaks down for the model due to the rapid oscillations of the scalar field. As a result, in what follows we will only focus on our new designer model, which does not suffer from this issue.

B. Designer model

We now focus on our designer model HDES, given by Eq. (169). Again, we will consider the numerical solutions for the following cases:

(i) The numerical solution of the full system of equations given by Eqs. (82)–(85), which, however, we rewrite in terms of $\delta X = \dot{\phi}\,\delta\dot{\phi} - \dot{\phi}^2\Psi$ as the system is more stable this way. We call this case "full-DES."

(ii) The numerical solution of the effective fluid approach given by Eqs. (16) and (17). We call this case "eff. fluid."

(iii) The numerical solution of the growth factor equation (101). We call this case "ODE-Geff."

(iv) The ΛCDM model.

As mentioned in the previous sections, we can absorb the constant c_0 in that of J_c, so we will only vary the latter; i.e., we set $\tilde{c}_0 = 1$. Furthermore, since the model is stable for all values of J_c when $n = 2$, we will consider this case when studying cosmological constraints. Again, we use $\Omega_{m,0} = 0.3$, $k = 300H_0$, and $\sigma_{8,0} = 0.8$, unless otherwise specified.

In the left panel of Fig. 4 we show the evolution of the $f\sigma_8(z)$ parameter for the HDES model with $n = 2$, $\tilde{J}_c = 5 \times 10^{-2}$, and $\sigma_{8,0} = 0.8$. The values of values for $\tilde{J}_c$ were chosen so as to highlight the differences of these models with respect to GR. We show the theoretical curves for the HDES model for the full-DES brute-force numerical solution, the effective fluid approach, the ΛCDM model, and the numerical solution of the $G_{\rm eff}$ equation. As can be seen, the agreement with all approaches is excellent. In the right panel of the same figure we show the percent difference between the full-DES brute-force numerical

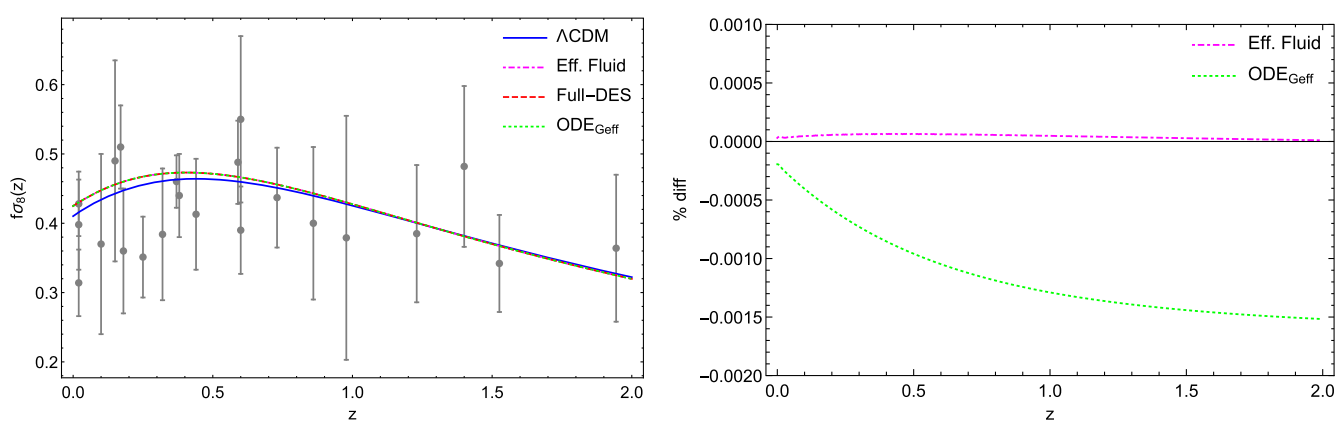

FIG. 4. Left: We show the evolution of the $f\sigma_8(z)$ parameter for the HDES model with $n = 2$, $\tilde{J}_c = 5 \times 10^{-2}$, and $\sigma_{8,0} = 0.8$ versus the $f\sigma_8$ data compilation from Ref. [88]. The values of values for $\tilde{J}_c$ were chosen so as to highlight the differences of these models with respect to GR. Here we show the theoretical curves for the HDES model for the "full-DES" brute-force numerical solution, the effective fluid approach, the ΛCDM model, and the numerical solution of the $G_{\rm eff}$ equation. As can be seen, the agreement with all approaches is excellent. Right: The percent difference between the full-DES brute-force numerical solution and the effective fluid approach (magenta dot-dashed line) and the numerical solution of the growth factor equation (101) (green dotted line).

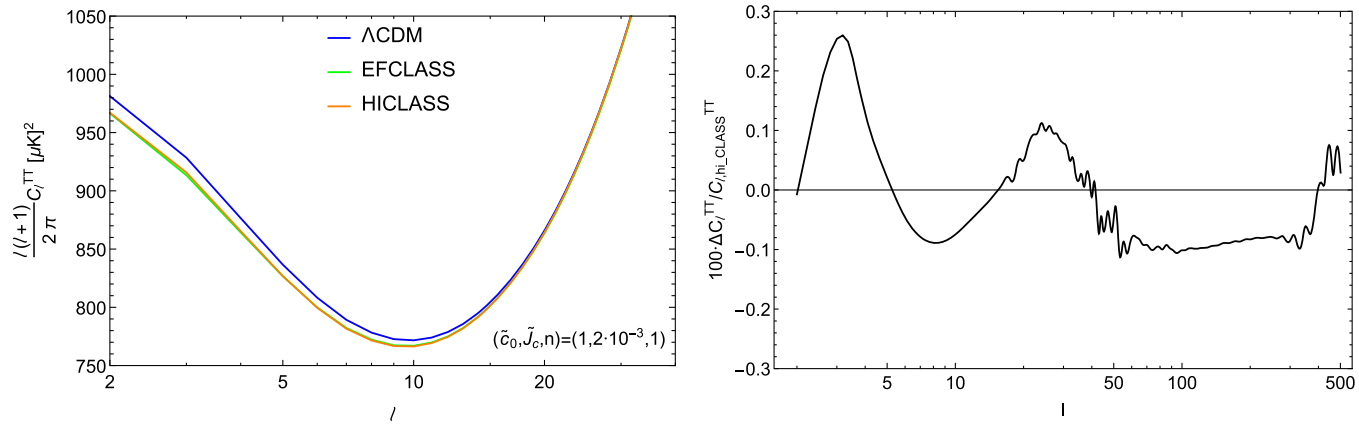

FIG. 5. Left: The low-ℓ multipoles of the TT CMB spectrum for a flat universe with $\Omega_{m,0} = 0.3$, $n_s = 1$, $A_s = 2.3 \times 10^{-9}$, $h = 0.7$, and $(\tilde{c}_0, \tilde{J}_c, n) = (1, 2 \times 10^{-3}, 1)$. The values of values for $\tilde{J}_c$ were chosen so as to highlight the differences of these models with respect to GR. Our EFCLASS code is denoted by the green line, HI_CLASS by the orange line, and for reference the ΛCDM with a blue line. Right: The percent difference of our code with HI_CLASS as a reference. As can be seen, our simple modification achieves roughly ∼0.1% accuracy across all multipoles.

solution and the effective fluid approach (magenta dot-dashed line) and the numerical solution of the growth factor equation (101) (green dotted line).

C. Modifications to CLASS and the ISW effect

Here we will present our modifications to the CLASS Boltzmann code, which we call EFCLASS. We will compare the outcome with the HI_CLASS code, which solves the full set of dynamical equations but at the cost of significantly more complicated modifications. At the same time, we will also compare with a brute-force calculation of the integrated Sachs-Wolfe (ISW) effect as in our previous paper [65].

In order to modify the CLASS code in our effective fluid approach we only need two functions, the DE velocity and the anisotropic stress [65]. In the case of the HDES model, the anisotropic stress π_{DE} is zero, as can be seen from Eq. (85), since $G_{4\phi} = 0$. Therefore, we only need the DE velocity which we can easily obtain from Eq. (119); however, we found that this approach is not very stable numerically. Hence, in order to have a consistent solution, we solve Eq. (17) for V_{DE}, and since $w_{\mathrm{DE}} = -1$, the only variable we need is the effective pressure δP_{DE} given by Eq. (117). The expressions are rather cumbersome, but for $n = 1$ we have

$$V_{\mathrm{DE}} \simeq \left(-\frac{14\sqrt{2}}{3}\Omega_{m,0}^{-3/4}\tilde{J}_c H_0 a^{1/4}\right)\frac{\bar{\rho}_m}{\bar{\rho}_{\mathrm{DE}}}\delta_m. \tag{187}$$

In the left panel of Fig. 5 we show the low-ℓ multipoles of the temperature CMB spectrum for a flat universe with $\Omega_{m,0} = 0.3$, $n_s = 1$, $A_s = 2.3 \times 10^{-9}$, $h = 0.7$, and $(\tilde{c}_0, \tilde{J}_c, n) = (1, 2 \times 10^{-3}, 1)$. Our EFCLASS code is denoted by the green line, HI_CLASS by the orange line,

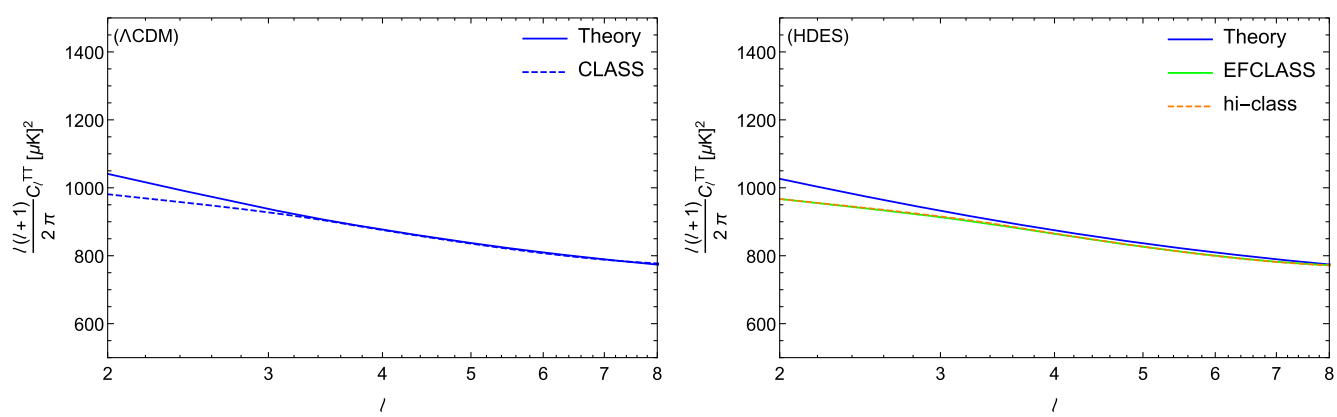

FIG. 6. The ISW effect and a comparison with CLASS/HI_CLASS for the ΛCDM model (left) and the HDES model (right), for the same parameters as in Fig. 5. We see that there is excellent agreement for all multipoles, except $\ell = 2$ due to the use of the BBKS transfer function which is accurate only up to 10% at large scales.

TABLE I. The $H(z)$ data used in the current analysis (in units of $\mathrm{km\,s^{-1}\,Mpc^{-1}}$). This compilation is partly based on those of Refs. [102,103].

z	$H(z)$	σ_H	Ref.
0.07	69.0	19.6	[104]
0.09	69.0	12.0	[105]
0.12	68.6	26.2	[104]
0.17	83.0	8.0	[105]
0.179	75.0	4.0	[106]
0.199	75.0	5.0	[106]
0.2	72.9	29.6	[104]
0.27	77.0	14.0	[105]
0.28	88.8	36.6	[104]
0.35	82.7	8.4	[107]
0.352	83.0	14.0	[106]
0.3802	83.0	13.5	[102]
0.4	95.0	17.0	[105]
0.4004	77.0	10.2	[102]
0.4247	87.1	11.2	[102]
0.44	82.6	7.8	[95]
0.44497	92.8	12.9	[102]
0.4783	80.9	9.0	[102]
0.48	97.0	62.0	[105]
0.57	96.8	3.4	[93]
0.593	104.0	13.0	[106]
0.60	87.9	6.1	[95]
0.68	92.0	8.0	[106]
0.73	97.3	7.0	[95]
0.781	105.0	12.0	[106]
0.875	125.0	17.0	[106]
0.88	90.0	40.0	[105]
0.9	117.0	23.0	[105]
1.037	154.0	20.0	[106]
1.3	168.0	17.0	[105]
1.363	160.0	33.6	[108]
1.43	177.0	18.0	[105]
1.53	140.0	14.0	[105]
1.75	202.0	40.0	[105]
1.965	186.5	50.4	[108]
2.34	222.0	7.0	[109]

and for reference the ΛCDM with a blue line. On the right panel of Fig. 5 we show the percent difference of our code with HI_CLASS as a reference.[7] As can be seen, our simple modification achieves roughly ∼0.1% accuracy across all multipoles.

We also compare our results with a brute-force calculation of the ISW effect. In this case the power spectrum is given by [89]

$$C_\ell^{\mathrm{ISW}} = 4\pi \int \frac{dk}{k} I_\ell^{\mathrm{ISW}}(k)^2 \frac{9}{25} \frac{k^3 P_\zeta}{2\pi^2}, \tag{188}$$

where $I_\ell^{\mathrm{ISW}}(k)$ is a kernel that depends on the line of sight integral of the growth and a bessel function, and P_ζ is the power spectrum (see Ref. [89] and Appendix A of Ref. [65]) and is given by the primordial power spectrum times a transfer function

$$\frac{k^3 P_\zeta}{2\pi^2} = A_s \left(\frac{k}{k_0}\right)^{n_s - 1} T(k)^2, \tag{189}$$

where A_s is the primordial amplitude, k_0 is the pivot scale, and $T(k)$ is the usual matter-radiation Bardeen-Bond-Kaiser-Szalay (BBKS) transfer function [see Eq. (7.71) in Ref. [90]].

In Fig. 6 we present the results for the calculation of the ISW effect and a comparison with CLASS/HI_CLASS for the ΛCDM model (left) and the HDES model (right), for the same parameters as in Fig. 5. We see that there is excellent agreement for all multipoles, except $\ell = 2$. The reason for this is that we have used the BBKS formula for the transfer function $T(k)$ which is very accurate at small scales, but only at the level of 10% on large scales, i.e., small multipoles.

TABLE II. Compilation of the $f\sigma_8(z)$ measurements used in this analysis along with the reference matter density parameter Ω_{m_0} (needed for the growth correction) and related references.

z	$f\sigma_8(z)$	$\sigma_{f\sigma_8}(z)$	$\Omega_{m,0}^{\mathrm{ref}}$	Ref.
0.02	0.428	0.0465	0.3	[115]
0.02	0.398	0.065	0.3	[116,117]
0.02	0.314	0.048	0.266	[117,118]
0.10	0.370	0.130	0.3	[119]
0.15	0.490	0.145	0.31	[120]
0.17	0.510	0.060	0.3	[111]
0.18	0.360	0.090	0.27	[121]
0.38	0.440	0.060	0.27	[121]
0.25	0.3512	0.0583	0.25	[122]
0.37	0.4602	0.0378	0.25	[122]
0.32	0.384	0.095	0.274	[123]
0.59	0.488	0.060	0.307115	[124]
0.44	0.413	0.080	0.27	[95]
0.60	0.390	0.063	0.27	[95]
0.73	0.437	0.072	0.27	[95]
0.60	0.550	0.120	0.3	[125]
0.86	0.400	0.110	0.3	[125]
1.40	0.482	0.116	0.27	[126]
0.978	0.379	0.176	0.31	[127]
1.23	0.385	0.099	0.31	[127]
1.526	0.342	0.070	0.31	[127]
1.944	0.364	0.106	0.31	[127]

[7]In this case we did not use $n = 2$ as we found that in this case HI_CLASS crashes and we cannot compare with that code.

VII. COSMOLOGICAL CONSTRAINTS

Here we present the cosmological constraints for the $n = 2$ HDES and ΛCDM models discussed in previous sections. We use the latest cosmological observations including the SnIa, baryon acoustic oscillations (BAO), CMB, and the Hubble expansion $H(z)$ data. Specifically, we use the Pantheon SnIa compilation of Ref. [91], the BAO measurements from 6dFGS [92], SDDS [93], BOSS CMASS [94], WiggleZ [95], MGS [96], BOSS DR12 [97], and DES Y1 [98]. For the CMB we use the shift parameters (R, l_a) based on the *Planck 2018* release [6] and as derived by Ref. [99]. We assume the existence of three families of neutrinos with $N_{\rm eff} = 3.046$.

Furthermore, we also incorporate the direct measurements of the Hubble expansion $H(z)$ data. These can be derived in two ways: by the clustering of galaxies or quasars and by the differential age method. The former provides direct measurements of the Hubble parameter by measuring the BAO peak in the radial direction from the clustering of galaxies or quasars [100]. The latter method obtains the Hubble parameter via the redshift drift of distant objects over significant time periods, usually a decade or longer. This is possible as in GR the Hubble parameter can be expressed via the rate of change of the redshift $H(z) = -\frac{1}{1+z}\frac{dz}{dt}$ [101]. These methods result in a compilation of 36 Hubble parameter $H(z)$ data points, which for clarity we show in Table I along with their corresponding references.

The growth-rate data used here are obtained via the redshift-space distortions (RSD). These are sensitive probes

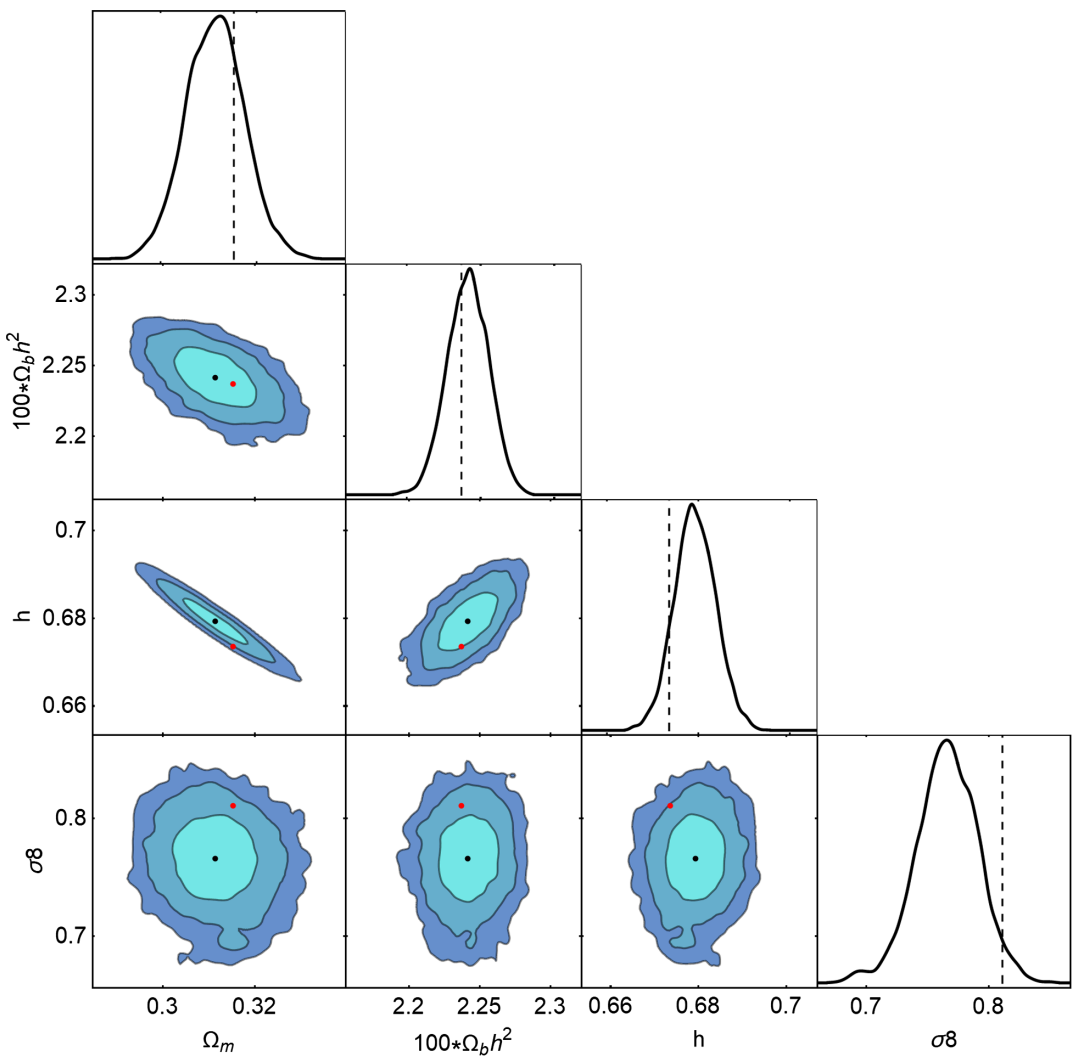

FIG. 7. The 68.3%, 95.4%, and 99.7% confidence contours for the ΛCDM model, along with the 1D marginalized likelihoods for all parameter combinations. We also highlight with a black point the mean MCMC values and with a red point or dashed vertical line the Planck 2018 concordance cosmology. The latter is based on the TT, TE, EE + lowP spectra, a flat ΛCDM model, and the values are shown in Table III.

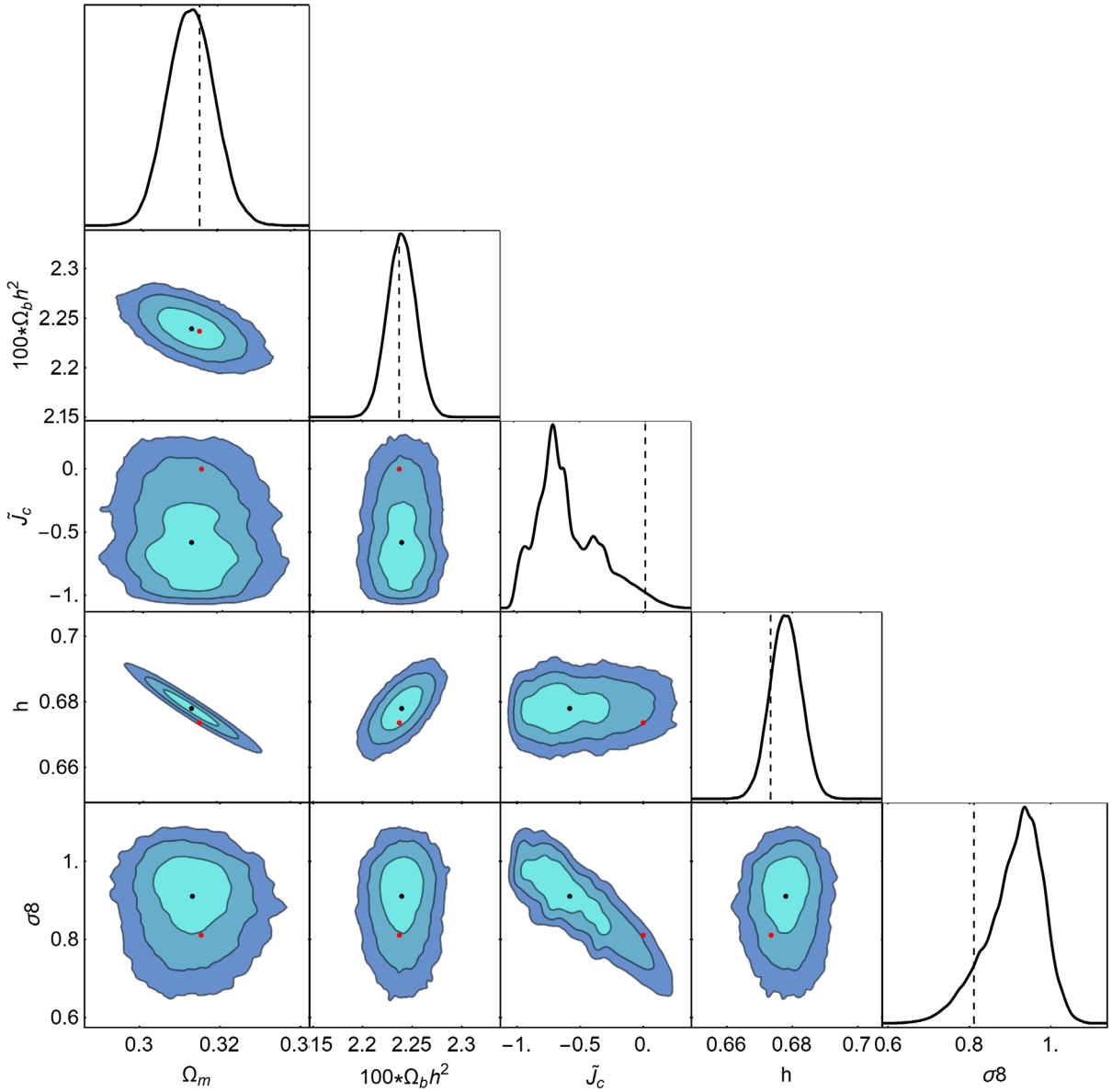

FIG. 8. The 68.3%, 95.4%, and 99.7% confidence contours for the HDES ($n = 2$) model, along with the 1D marginalized likelihoods for all parameter combinations. We also highlight with a black point the mean MCMC values and with a red point or dashed vertical line the Planck 2018 concordance cosmology. The latter is based on the TT, TE, EE + lowP spectra, a flat ΛCDM model, and the values are shown in Table III.

of the large scale structure (LSS) and can measure the quantity $f\sigma_8(a) \equiv f(a) \cdot \sigma(a)$, which is a product of the growth rate $f(a) = \frac{d\ln\delta}{d\ln a}$ and the redshift-dependent rms fluctuations $\sigma(a) = \sigma_{8,0}\frac{\delta(a)}{\delta(1)}$ of the linear density field within spheres of radius $R = 8h^{-1}$ Mpc. In this notation the parameter $\sigma_{8,0}$ is the value of the rms fluctuations today and is a direct measure of the amplitude of fluctuations in linear scales.

We should mention that $f\sigma_8(a)$ can be estimated via the ratio of the monopole to the quadrupole of the redshift-space power spectrum $P(k)$. The latter is sensitive on the quantity $\beta = f/b_1$, where f is the growth rate as defined earlier and

TABLE III. ΛCDM parameters with 68% limits based on TT, TE, EE + lowP and a flat ΛCDM model (middle column) or a wCDM model (right column); see Ref. [6] and the Planck chains archive.

Parameter	Value (ΛCDM)	Value (wCDM)
$\Omega_b h^2$	0.02225 ± 0.00016	0.02229 ± 0.00016
$\Omega_c h^2$	0.1198 ± 0.0015	0.1196 ± 0.0015
n_s	0.9645 ± 0.0049	0.9649 ± 0.0048
H_0	67.27 ± 0.66	>81.3
Ω_m	0.3156 ± 0.0091	$0.203^{+0.022}_{-0.065}$
w	-1	$-1.55^{+0.19}_{-0.38}$
σ_8	0.831 ± 0.013	$0.983^{+0.100}_{-0.055}$

TABLE IV. The best-fit parameters for the ΛCDM and the HDES ($n = 2$) models, respectively.

Model	$\Omega_{m,0}$	$100\Omega_b h^2$	$\tilde{J}_c$	h	σ_8
Best-fit values					
ΛCDM	0.311 ± 0.006	2.243 ± 0.014	0	0.680 ± 0.004	0.758 ± 0.025
HDES	0.313 ± 0.006	2.240 ± 0.014	-0.309 ± 0.244	0.678 ± 0.004	0.911 ± 0.068

b_1 is the galaxy bias [110–112]. In all cases we assume linear theory. The combination $f\sigma_8(a)$ not only is independent of bias, as the latter completely cancels out, but it has also been demonstrated to be an excellent discriminator of DE models as it probes the dynamics of a given gravitational theory and not only the geometric of spacetime [111]. The covariances of the data and how to make the necessary corrections for the Alcock-Paczynski effect are given in Refs. [27,88,113], while other related analyses with these data can be found in Refs. [24,26,28,65].

In this paper we use the growth-rate data compilation of Ref. [88], which we show in Table II for completeness, along with the corresponding references for each point. This dataset was analyzed in Ref. [88] with the 'internal robustness method" of Ref. [114], by examining combinations of subsets, and it was shown that this specific dataset is indeed internally robust.

With these in mind, our total likelihood function $L_{\rm tot}$ can be given as the product of the separate likelihoods of the data (we assume they are statistically independent) as follows:

$$L_{\rm tot} = L_{\rm SnIa} \times L_{\rm BAO} \times L_{\rm H(z)} \times L_{\rm CMB} \times L_{\rm growth},$$

which is related to the total χ^2 via $\chi^2_{\rm tot} = -2\log L_{\rm tot}$ or

$$\chi^2_{\rm tot} = \chi^2_{\rm SnIa} + \chi^2_{\rm BAO} + \chi^2_{\rm H(z)} + \chi^2_{\rm cmb} + \chi^2_{\rm growth}. \qquad (190)$$

Calculating the best fit is not enough, but we also need to study the statistical significance of our constraints. To achieve this we make use of the well known Akaike information criterion (AIC) [128]. The AIC estimator is given (assuming Gaussian errors) by

$$\mathrm{AIC} = -2\ln\mathcal{L}_{\rm max} + 2k_p + \frac{2k_p(k_p+1)}{N_{\rm dat} - k_p - 1}, \qquad (191)$$

where k_p and $N_{\rm dat}$ stand for the number of free parameters and the total number of data points, respectively. For other similar statistical tools see also Ref. [129]. In this analysis we have 1048 data points from the Pantheon set, 3 from the CMB shift parameters, 10 from the BAO measurements, 22 from the growth measurements, and finally 36 $H(z)$ points, for a total of $N_{\rm dat} = 1118$.

TABLE V. The χ^2 and AIC parameters for the ΛCDM and the HDES models, respectively.

Model	χ^2	AIC	ΔAIC
ΛCDM	1087.64	1095.68	0
HDES	1086.30	1096.35	0.678

The AIC can be interpreted similarly to the χ^2; i.e., a smaller relative value signifies a better fit to the data. To apply this statistic to model selection we take the pair difference between models $\Delta\mathrm{AIC} = \mathrm{AIC}_{\rm model} - \mathrm{AIC}_{\rm min}$. This can in principle be interpreted with the Jeffreys' scale in the following manner: when $4 < \Delta\mathrm{AIC} < 7$, this indicates positive evidence against the model with a higher value of $\mathrm{AIC}_{\rm model}$, while in the case when $\Delta\mathrm{AIC} \geq 10$ it can be interpreted as strong evidence. On the other hand, when $\Delta\mathrm{AIC} \leq 2$, then this means that the two models are statistically equivalent. However, in Ref. [130] it has been shown that in general the Jeffreys' scale can sometimes lead to misleading conclusions, and thus it should be interpreted with care.

Finally, our total χ^2 is given by Eq. (190) while the parameter vectors (assuming a spatially flat Universe) are given by $p_{\Lambda\rm CDM} = (\Omega_{m,0}, 100\Omega_b h^2, h, \sigma_8)$ for the ΛCDM and $p_{\rm HDES} = (\Omega_{m,0}, 100\Omega_b h^2, h, \tilde{J}_c, \sigma_8)$ for the HDES model. Using the aforementioned cosmological data and methodology, we can obtain the best-fit parameters and their uncertainties via the MCMC method based on a Metropolis-Hastings algorithm. The codes used in the analysis were written by one of the authors.[8] The priors we assumed for the parameters are given by $\Omega_{m,0} \in [0.1, 0.5]$, $\Omega_b h^2 \in [0.001, 0.08]$, $\tilde{J}_c \in [-1, 12]$, $h \in [0.4, 1]$, $\sigma_8 \in [0, 2]$, and we sample $\sim 10^5$ MCMC points for each of the two models.

A. Results

In Figs. 7 and 8 we show the 68.3%, 95.4%, and 99.7% confidence contours for the ΛCDM and the HDES models, respectively, along with the one-dimensional (1D) marginalized likelihoods for all parameter combinations in the familiar triangle plot. We also highlight with a black point the mean MCMC values and with a red point the Planck 2018 concordance cosmology. The latter is based on the TT, TE, EE + lowP spectra, a flat ΛCDM model, and the values are shown in Table III.

[8]The MCMC code for *Mathematica* used in the analysis is freely available at http://members.ift.uam-csic.es/savvas.nesseris/.

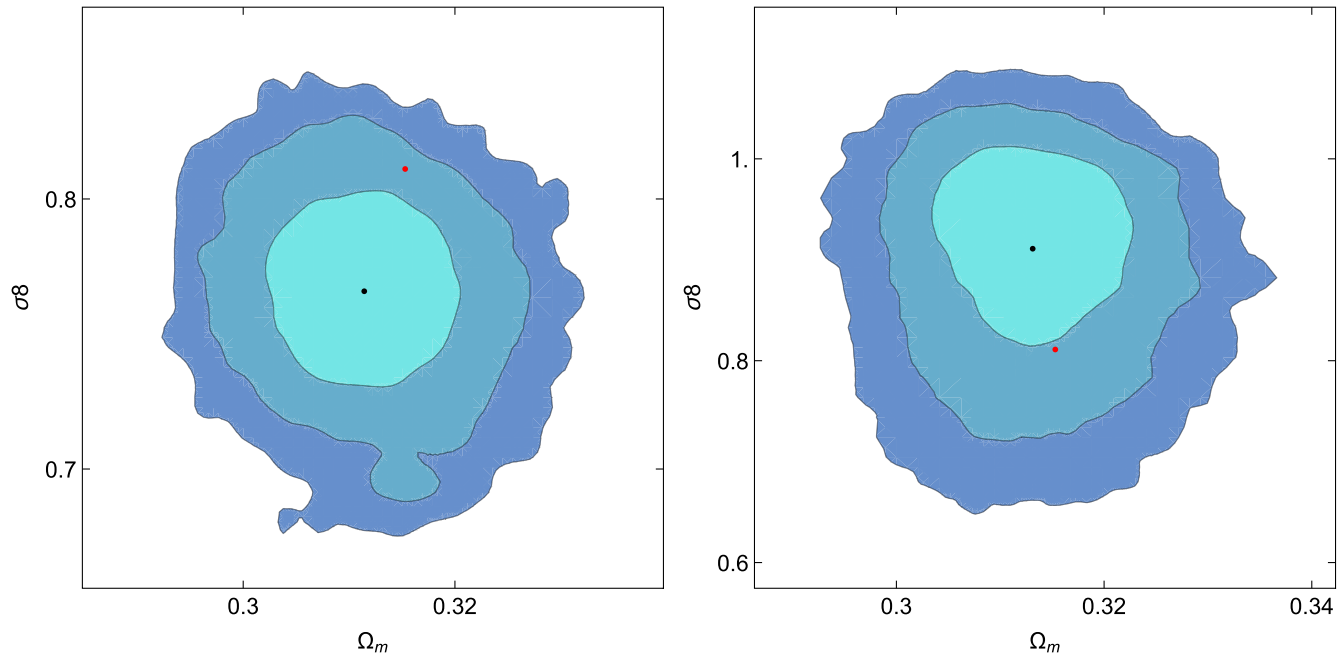

FIG. 9. The 68.3%, 95.4%, and 99.7% confidence contours for the ΛCDM (left) and the HDES ($n = 2$) (right) models, respectively, in the $(\Omega_{m,0}, \sigma_8)$ plane. We also highlight with a black point the mean MCMC values and with a red point or dashed vertical line the Planck 2018 concordance cosmology. The latter is based on the TT, TE, EE + lowP spectra, a flat ΛCDM model and the values are shown in Table III.

In Tables IV and V we show the best-fit values of the model parameters and the values for the χ^2 and AIC parameters for the ΛCDM and the HDES model, respectively. As can be seen from Tables IV and V, we find that as the difference in the AIC parameters is roughly ∼0.68, then both models seem to be statistically equivalent with each other. Furthermore, as seen in Fig. 8, there is a clear negative correlation between $\tilde{J}_c$ and σ_8 as we saw in Sec. V E and Eq. (183) due to the strong degeneracy between the parameters. This degeneracy is useful as it can potentially alleviate and relax the tension that has been recently observed, see Refs. [27,88]. In particular, in Fig 9 we show the 68.3%, 95.4%, and 99.7% confidence contours for the ΛCDM (left) and the HDES ($n = 2$) (right) models, respectively, in the $(\Omega_{m,0}, \sigma_8)$ plane. As can be seen, for the HDES model, the best fit in the $(\Omega_{m,0}, \sigma_8)$ plane moves toward higher values of σ_8, closer to those of Planck.

VIII. CONCLUSIONS

The recent discovery of gravitational waves emission from a binary neutron star merger with an optical counterpart, signified a major breakthrough in astrophysics and cosmology as it provided a direct measurement of the speed of propagation of gravitational waves. This observation not only represented an important advance for astronomy, but it also served to greatly reduce the number of alternative models aiming at explaining the current accelerating phase of the Universe. In particular, since the constraint on the speed of propagation of gravitational waves is extremely close to the speed of light, the Horndeski Lagrangian simplified to only three functions. Although this means a notable progress in constraining cosmological models, degeneracies with the ΛCDM model remain and must be further investigated.

In this paper we used an effective fluid approach to study the remaining Horndeski Lagrangian. This formalism makes it possible to compare models with different underlying physics (e.g., DE and MG models) in a relatively easy way: each model is mapped to three functions describing the effective fluid, namely, the equation of state w, the sound speed c_s^2, and the anisotropic stress π. Even though the remaining Horndeski Lagrangian is now simpler than its original version, finding exact analytical solutions can be quite laborious. Nevertheless, the subhorizon and quasistatic approximations are pretty helpful at overcoming this difficulty.

One of our main results is the set of Eqs. (102)–(107). These equations along with the equation of state Eq. (73) describe the remaining Horndeski Lagrangian in an effective fluid approach under the subhorizon and quasistatic approximations. In this paper, we provide explicit expressions for the effective fluid description of several DE and MG models.

In order to exemplify our results and since we focused on explanations to the late-time accelerating universe, we carried out an analysis where only DM and an effective DE

fluid are taken into consideration. A particularly interesting model also included in our formalism is the KGB model. In Sec. VI we show our analytical solutions agree pretty well with a full numerical solution of the system of differential equations describing the DM and effective DE perturbations. We also confirm that the subhorizon approximation breaks down for the KGB model due to the rapid oscillations of the scalar field in the large n limit, in agreement with Ref. [79]. Also, for the KGB model the background equation for the expansion history $H(a)$ can only be found numerically for $n > 1$, thus slowing down the codes significantly.

Due to these problems, we propose a completely new class of Horndeski models based on the designing principle, i.e., fixing the background to a specific model, usually that of the ΛCDM and then determining the Lagrangian. Given the freedom in specifying the remaining functions of the Horndeski Lagrangian, we propose a way to find families of models which match a particular background expansion, i.e., the equation of state $w_{\rm DE}$. Since current observations are in good agreement with the standard ΛCDM at the background level, we provide equations specifying a $w_{\rm DE} = -1$ designer Horndeski model [see Eqs. (169)], which we call HDES. Furthermore, for this model we are able to find exact solutions for the growth $\delta_m(a)$ in the matter domination epoch by solving Eq. (101). The solutions we found are given by Eq. (179), and they imply a degeneracy between σ_8 and the parameter of the HDES model $\tilde{J}_c$, which can approximately be described via Eq. (183).

Although fixing the background to ΛCDM is a common practice, the treatment of the perturbations might not be rigorous enough in current studies. Public codes solving the perturbation equations for the Horndeski Lagrangian (e.g., HI_CLASS) use *ad hoc* parametrizations for the α_i functions which differ significantly from our findings that approximate a realistic model [see Eqs. (171)–(175)]; see, for example, Refs. [131–133].

We implemented the parametrized version for the DE effective fluid of our $w_{\rm DE} = -1$ designer Horndeski HDES model in the public code CLASS, which we call EFCLASS, by following the straightforward implementation explained in our previous paper [65]. For the sake of comparison and in order to check the validity of our effective fluid approach, we compared results from our code EFCLASS with the public code HI_CLASS, which solves numerically the full perturbation equations.

In Fig. 5 we show the CMB angular power spectrum computed with both codes, and as can be seen in the right panel of Fig. 5, the agreement is remarkable and on average on the order of ∼0.1%. Since the HI_CLASS code does not utilize either the subhorizon or the quasistatic approximation, but our EFCLASS does it, we conclude our effective fluid approach is quite accurate and powerful. Furthermore, the main advantage of our method is that while HI_CLASS requires significant and nontrivial modifications, our EFCLASS code practically only requires the implementation of Eq. (187), which is trivial.

We further investigated our $w_{\rm DE} = -1$ designer Horndeski HDES model by computing cosmological constraints with recent datasets using an MCMC analysis. The results of our MCMC analysis are shown in Tables IV and V, where we present the best-fit values of the model parameters and the values for the χ^2 and AIC parameters for the ΛCDM and the HDES model, respectively. We find that as the difference in the AIC parameters is roughly ∼0.68, then both models seem to be statistically equivalent with each other. Furthermore, as seen in Fig. 8, there is a clear negative correlation between $\tilde{J}_c$ and σ_8. This can be understood, as we saw in Sec. V E, due to the strong degeneracy between the parameters described by Eq. (183). This degeneracy is useful as it can potentially alleviate the σ_8 tension that has been recently observed; see Refs. [27,88].

Numerical analysis files: The numerical codes used by the authors in the analysis of the paper and our modifications to the CLASS code, which we call EFCLASS, will be released upon publication of the paper on the websites of the EFCLASS https://members.ift.uam-csic.es/savvas.nesseris/efclass.html and https://github.com/wilmarcardonac/EFCLASS.

ACKNOWLEDGMENTS

The authors thank Hector Gil Marín and Tomás Ortín for useful discussions. They also acknowledge support from the Research Projects No. FPA2015-68048-03-3P [MINECO-FEDER] and No. PGC2018-094773-B-C32 and the Centro de Excelencia Severo Ochoa Program SEV-2016-0597. S. N. also acknowledges support from the Ramón y Cajal program through Grant No. RYC-2014-15843.

APPENDIX A: SCALAR AND GRAVITATIONAL FIELD EQUATIONS

For completeness, in this appendix we show how to compute both the gravitational and the scalar-field equations derived from the Horndeski action (21).

1. Scalar field equation

For a function of a single variable with higher derivatives, the stationary values of the functional [134]

$$I[f] = \int_{x_0}^{x_1} \mathcal{L}(x, f, f', f'', \ldots, f^{(k)})dx; \qquad f' \equiv \frac{df}{dx},$$
$$f'' \equiv \frac{d^2 f}{dx^2}, \qquad f^{(k)} \equiv \frac{d^k f}{dx^k}, \tag{A1}$$

can be obtained from the Euler-Lagrange equation

$$\frac{\partial \mathcal{L}}{\partial f} - \frac{d}{dx}\left(\frac{\partial \mathcal{L}}{\partial f'}\right) + \frac{d^2}{dx^2}\left(\frac{\partial \mathcal{L}}{\partial f''}\right) - \cdots (-1)^k \frac{d^k}{dx^k}\left(\frac{\partial \mathcal{L}}{\partial f^k}\right) = 0. \tag{A2}$$

Since our Lagrangian $\mathcal{L}_i$ functions defined in the Horndeski action (21) depend on the scalar field ϕ and its first and second derivatives, we can use the Euler-Lagrange equation (A2) to compute the scalar field equation for $\mathcal{L}_2$, $\mathcal{L}_3$, and $\mathcal{L}_4$. For $\mathcal{L}_2$ we have

$$\mathcal{L}_2(\phi, \partial_\mu\phi) = \frac{\partial \mathcal{L}_2}{\partial \phi}\delta\phi + \frac{\partial \mathcal{L}_2}{\partial_\mu \phi}\delta(\partial_\mu\phi) = \frac{\partial \mathcal{L}_2}{\partial \phi}\delta\phi - \partial_\mu \frac{\partial \mathcal{L}_2}{\partial_\mu \phi}\delta\phi, \tag{A3}$$

$$\frac{\partial \mathcal{L}_2}{\partial \phi} - \partial_\mu \frac{\partial \mathcal{L}_2}{\partial_\mu \phi} = P^2_\phi - \nabla^\mu J^2_\mu = 0. \tag{A4}$$

Since $\mathcal{L}_2 = K(\phi, X)$, applying Eq. (A4) leads to

$$P^2_\phi = \frac{\partial \mathcal{L}_2}{\partial \phi} = K_\phi, \tag{A5}$$

$$\nabla^\mu J^2_\mu = \partial_\mu \frac{\partial \mathcal{L}_2}{\partial_\mu \phi} = \nabla^\mu\left(\frac{\partial K}{\partial^\mu \phi}\right) = \nabla^\mu\left(\frac{\partial K}{\partial X}\frac{\partial X}{\partial^\mu \phi}\right) = -\nabla^\mu(K_X \nabla_\mu \phi), \tag{A6}$$

where we have replaced the partial derivatives by covariant derivatives and we are using the fact that $X = -\frac{1}{2}\partial_\mu\phi\partial^\mu\phi$. Hence, for $\mathcal{L}_2$ the scalar field equation reads

$$K_\phi + \nabla^\mu(K_X \nabla_\mu \phi) = 0. \tag{A7}$$

For the term $\mathcal{L}_3$ we follow the same approach,

$$\mathcal{L}_3(\phi, \partial_\mu\phi, \partial_\mu\partial_\nu\phi) = \frac{\partial \mathcal{L}_3}{\partial \phi}\delta\phi + \frac{\partial \mathcal{L}_3}{\partial_\mu \phi}\delta(\partial_\mu\phi) + \frac{\partial \mathcal{L}_3}{\partial_\mu\partial_\nu \phi}\delta(\partial_\mu\partial_\nu\phi) = \frac{\partial \mathcal{L}_3}{\partial \phi}\delta\phi - \partial_\mu \frac{\partial \mathcal{L}_3}{\partial_\mu \phi}\delta\phi + \partial_\mu\partial_\nu \frac{\partial \mathcal{L}_3}{\partial_\mu\partial_\nu \phi}\delta\phi, \tag{A8}$$

$$\frac{\partial \mathcal{L}_3}{\partial \phi} - \partial_\mu \frac{\partial \mathcal{L}_3}{\partial_\mu \phi} + \partial_\mu\partial_\nu \frac{\partial \mathcal{L}_3}{\partial_\mu\partial_\nu \phi} = 0. \tag{A9}$$

Knowing that $\mathcal{L}_3 = -G_3(\phi, X)$ $[\Box\phi = g^{\mu\nu}\nabla_\mu\nabla_\nu\phi]$, applying Eq. (A9) gives

$$\frac{\partial \mathcal{L}_3}{\partial \phi} = -G_{3\phi}\Box\phi, \tag{A10}$$

$$\partial_\mu \frac{\partial \mathcal{L}_3}{\partial_\mu \phi} = \nabla^\mu\left(\frac{\partial G_3}{\partial^\mu \phi}\Box\phi\right) = \nabla^\mu\left(\frac{\partial G_3}{\partial X}\frac{\partial X}{\partial^\mu \phi}\Box\phi\right) = -\nabla^\mu(G_{3X}\nabla_\mu\phi\Box\phi), \tag{A11}$$

$$\partial_\mu\partial_\nu \frac{\partial \mathcal{L}_3}{\partial_\mu\partial_\nu \phi} = -\nabla_\mu(\nabla_\nu g^{\mu\nu} G_3) = -\nabla^\mu(G_{3\phi}\nabla_\mu\phi + G_{3X}\nabla_\mu X), \tag{A12}$$

where we have replaced again the partial derivatives by covariant derivatives. We can then conclude that for $\mathcal{L}_3$ the scalar field equation reads

$$-G_{3\phi}\Box\phi - \nabla^\mu(G_{3X}\nabla_\mu\phi\Box\phi) - \nabla^\mu(G_{3\phi}\nabla_\mu\phi) - \nabla^\mu(G_{3X}\nabla_\mu X) = 0, \tag{A13}$$

and we make the following assignment:

$$P^3_\phi = \nabla_\mu G_{3\phi}\nabla^\mu\phi, \tag{A14}$$

$$\nabla^\mu J^3_\mu = \nabla^\mu(-G_{3X}\nabla_\mu\phi + G_{3X}\nabla_\mu X + 2G_{3\phi}\nabla_\mu\phi). \tag{A15}$$

For $\mathcal{L}_4$ we have

$$\mathcal{L}_4(\phi) = \frac{\partial \mathcal{L}_4}{\partial \phi}\delta\phi, \tag{A16}$$

$$\frac{\partial \mathcal{L}_4}{\partial \phi} = P^4_\phi = 0. \tag{A17}$$

Since $\mathcal{L}_4 = G_4(\phi)R$, applying Eq. (A17) leads to

$$P^4_\phi = G_{4\phi}R. \tag{A18}$$

Our result for the scalar field equation considering $G_{4X} = 0$ and $G_5 = 0$ is in full agreement with Ref. [73]. Hence, the scalar-field equation can be written as

$$\nabla^\mu\left(\sum_{i=2}^{4} J^i_\mu\right) = \sum_{i=2}^{4} P^i_\phi. \tag{A19}$$

2. Gravitational field equations

Defining the arbitrary functions $\mathcal{L}_i$ from the action (21) as

$$\mathcal{L}_2 = K(\phi, X), \tag{A20}$$

$$\mathcal{L}_3 = -G_3(\phi, X)\Box\phi, \tag{A21}$$

$$\mathcal{L}_4 = G_4(\phi)R, \tag{A22}$$

we can then vary the action with respect to the metric tensor; using the principle of least action, this leads to

$$\delta S = \delta S_2 + \delta S_3 + \delta S_4 + \delta(\sqrt{-g}\mathcal{L}_m) = 0. \tag{A23}$$

For δS_2 we have

$$\delta S_2 = \int d^4x[\delta\sqrt{-g}K + \sqrt{-g}\delta K], \tag{A24}$$

and using the fact that

$$\delta\sqrt{-g} = -\frac{1}{2}\sqrt{-g}g_{\mu\nu}\delta g^{\mu\nu}, \tag{A25}$$

and that the variation of K with respect to the metric can be written as

$$\delta K(\phi, X) = K_X\delta g^{\mu\nu}\left(-\frac{1}{2}\nabla_\mu\phi\nabla_\nu\phi\right), \tag{A26}$$

we get

$$\delta S_2 = \int d^4x\sqrt{-g}\delta g^{\mu\nu}\left[-\frac{1}{2}Kg_{\mu\nu} - \frac{1}{2}K_X\nabla_\mu\phi\nabla_\nu\phi\right]. \tag{A27}$$

For δS_3 we have

$$\delta S_3 = \int d^4x[-\delta\sqrt{-g}G_3\Box\phi - \sqrt{-g}\delta(G_3\Box\phi)]. \tag{A28}$$

The variations of G_3 with respect to the metric can be written as

$$\begin{aligned}\delta(G_3(\phi, X)\Box\phi) &= \delta G_3\Box\phi + G_3\delta(\Box\phi)\\ &= G_{3X}\delta g^{\mu\nu}\left(-\frac{1}{2}\nabla_\mu\phi\nabla_\nu\phi\right)\Box\phi\\ &\quad + G_3\delta(\Box\phi);\end{aligned} \tag{A29}$$

hence

$$\begin{aligned}\delta S_3 = \int d^4x\sqrt{-g}\Big[&\frac{1}{2}g_{\mu\nu}\delta g^{\mu\nu}G_3\Box\phi\\ &+ \frac{1}{2}\delta g^{\mu\nu}G_{3X}\Box\phi\nabla_\mu\phi\nabla_\nu\phi + G_3\delta(\Box\phi)\Big].\end{aligned} \tag{A30}$$

The last term of the above equation can be expanded in the following way:

$$\begin{aligned}\delta\Box\phi &= \delta g^{ab}\nabla_a\nabla_b\phi + g^{ab}\delta(\nabla_a\nabla_b\phi)\\ &= \delta g^{ab}\nabla_a\nabla_b\phi + \Box(\delta\phi) - g^{ab}\delta\Gamma^\gamma_{ab}\partial_\gamma\phi,\end{aligned} \tag{A31}$$

since

$$\nabla_a\nabla_b\phi = \partial_a\partial_b\phi - \Gamma^\gamma_{ab}\partial_\gamma\phi \tag{A32}$$

and

$$\delta(\nabla_a\nabla_b\phi) = \nabla_a\nabla_b(\delta\phi) - \delta\Gamma^\gamma_{ab}\partial_\gamma\phi. \tag{A33}$$

Also we have that $g^{ab}\Gamma^\gamma_{ab} = \cdots = -\nabla_a\delta g^{\gamma a} + \frac{1}{2}g_{ab}g^{\gamma\lambda}\nabla_\lambda\delta g^{ab}$, so we get for the last term in Eq. (A30)

$$\begin{aligned}\delta S_{\text{last-term}} &= \int d^4x\sqrt{-g}(-G_3)\left(\delta g^{ab}\nabla_a\nabla_b\phi + \Box\delta\phi + \left(\nabla_a\delta g^{\gamma a} - \frac{1}{2}g_{ab}g^{\gamma\lambda}\nabla_\lambda\delta g^{ab}\right)\partial_\gamma\phi\right)\\ &= \int d^4x\sqrt{-g}\left[-\delta g^{\mu\nu}(\nabla_\mu\nabla_\nu)G_3 + \delta g^{\gamma a}\nabla_a(G_3\nabla_\gamma\phi) - \frac{1}{2}\delta g^{ab}g_{ab}g^{\gamma\lambda}\nabla_\lambda(G_3\nabla_\gamma\phi)\right]\\ &= \int d^4x\sqrt{-g}\left[-\delta g^{\mu\nu}(\nabla_\mu\nabla_\nu)G_3 + \delta g^{\mu\nu}\nabla_\nu(G_3\nabla_\mu\phi) - \frac{1}{2}\delta g^{\mu\nu}g_{\mu\nu}\nabla^\gamma(G_3\nabla_\gamma\phi)\right]\\ &= \int d^4x\sqrt{-g}\delta g^{\mu\nu}\left[(\nabla_{(\mu}\phi)(\nabla_{\nu)}G_3) - \frac{1}{2}g_{\mu\nu}\nabla^\gamma(G_3\nabla_\gamma\phi)\right].\end{aligned} \tag{A34}$$

Combining all terms we have

$$\delta S_3 = \int d^4x\sqrt{-g}\delta g^{\mu\nu}\left[\frac{1}{2}G_{3X}\Box\phi\nabla_\mu\phi\nabla_\nu\phi + \nabla_{(\mu}G_3\nabla_{\nu)}\phi - \frac{1}{2}g_{\mu\nu}\nabla_\lambda G_3\nabla^\lambda\phi\right]. \tag{A35}$$

For δS_4 we have

$$\delta S_4 = \int d^4x[\delta\sqrt{-g}G_4R + \sqrt{-g}G_4\delta R], \tag{A36}$$

where

$$\begin{aligned}\delta R &= \delta(g^{\mu\nu}R_{\mu\nu})\\ &= R_{\mu\nu}\delta g^{\mu\nu} + g^{\mu\nu}\delta R_{\mu\nu}\\ &= R_{\mu\nu}\delta g^{\mu\nu} + g^{\mu\nu}(\nabla_\rho\delta\Gamma^\rho_{\nu\mu} - \nabla_\nu\delta\Gamma^\rho_{\rho\mu}).\end{aligned} \tag{A37}$$

Since $\delta\Gamma^\lambda_{\mu\nu}$ is the difference of two connections, it should transform as a tensor. Therefore, it can be written as

$$\delta\Gamma^\lambda_{\mu\nu} = \frac{1}{2}g^{\lambda\alpha}(\nabla_\mu\delta g_{\alpha\nu} + \nabla_\nu\delta g_{\alpha\mu} - \nabla_\alpha\delta g_{\mu\nu}). \tag{A38}$$

Then, substituting Eq. (A38) into (A37), we get

$$\delta R = R_{\mu\nu}\delta g^{\mu\nu} + g_{\mu\nu}\Box(\delta g^{\mu\nu}) - \nabla_\mu\nabla_\nu(\delta g^{\mu\nu}); \tag{A39}$$

hence

$$\begin{aligned}\delta S_4 &= \int d^4x\sqrt{-g}\left[-\frac{1}{2}g_{\mu\nu}\delta g^{\mu\nu}G_4R + G_4R_{\mu\nu}\delta g^{\mu\nu} + G_4(g_{\mu\nu}\Box(\delta g^{\mu\nu}) - \nabla_\mu\nabla_\nu(\delta g^{\mu\nu}))\right]\\ &= \int d^4x\sqrt{-g}\delta g^{\mu\nu}[G_{\mu\nu}G_4 + g_{\mu\nu}\Box G_4 - \nabla_\mu\nabla_\nu G_4 + \text{total derivatives}]\\ &= \int d^4x\sqrt{-g}\delta g^{\mu\nu}[G_{\mu\nu}G_4 + g_{\mu\nu}(G_{4\phi}\Box\phi - 2XG_{4\phi\phi}) - G_{4\phi}\nabla_\mu\nabla_\nu\phi - G_{4\phi\phi}\nabla_\mu\phi\nabla_\nu\phi + \text{total derivatives}],\end{aligned} \tag{A40}$$

where

$$\begin{aligned}-\nabla_\mu(\nabla_\nu G_4) &= -\nabla_\mu(\nabla_\nu\phi G_{4\phi})\\ &= -\nabla_\mu\nabla_\nu\phi G_{4\phi} - \nabla_\mu\phi\nabla_\nu\phi G_{4\phi\phi},\end{aligned} \tag{A41}$$

$$\begin{aligned}g_{\mu\nu}\Box G_4 &= g_{\mu\nu}(g^{ab}\nabla_a\nabla_b G_4)\\ &= g_{\mu\nu}(g^{ab}\nabla_a(\nabla_b\phi G_{4\phi}))\\ &= g_{\mu\nu}(g^{ab}\nabla_a\nabla_b\phi G_{4\phi} + g^{ab}\nabla_b\phi\nabla_a G_{4\phi})\\ &= g_{\mu\nu}(\Box\phi G_{4\phi} - 2XG_{4\phi\phi}).\end{aligned} \tag{A42}$$

Since the energy-momentum tensor is defined as

$$T^{(m)}_{\mu\nu} = -\frac{2}{\sqrt{-g}}\frac{\delta(\sqrt{-g}\mathcal{L}_m)}{\delta g^{\mu\nu}}, \tag{A43}$$

the gravitational field equation can be written

$$\begin{aligned}T^{(m)}_{\mu\nu} &= -K_X\nabla_\mu\phi\nabla_\nu\phi - Kg_{\mu\nu} + G_{3X}\Box\phi\nabla_\mu\phi\nabla_\nu\phi\\ &\quad + 2\nabla_{(\mu}G_3\nabla_{\nu)}\phi - g_{\mu\nu}\nabla_\lambda G_3\nabla^\lambda\phi + 2G_4G_{\mu\nu}\\ &\quad + 2g_{\mu\nu}(G_{4\phi}\Box\phi - 2XG_{4\phi\phi}) - 2G_{4\phi}\nabla_\mu\nabla_\nu\phi\\ &\quad - 2G_{4\phi\phi}\nabla_\mu\phi\nabla_\nu\phi.\end{aligned} \tag{A44}$$

APPENDIX B: COEFFICIENTS

Here we show the coefficients for the perturbations in the Horndeski theory in Eq. (21). They are given by

$$A_1 = -3\dot\phi^3G_{3X} + 12HG_4 + 6\dot\phi G_{4\phi}, \tag{B1}$$

$$\begin{aligned}A_2 &= -\dot\phi(K_X + \dot\phi^2K_{XX}) + 2\dot\phi G_{3\phi}\\ &\quad - 3H\dot\phi^2(3G_{3X} + \dot\phi^2G_{3XX}) + \dot\phi^3G_{3\phi X}\\ &\quad + 6HG_{4\phi},\end{aligned} \tag{B2}$$

$$A_3 = 4G_4, \tag{B3}$$

$$\begin{aligned}A_4 &= \dot\phi^2(K_X + \dot\phi^2K_{XX}) - 2\dot\phi^2G_{3\phi} - \dot\phi^4G_{3\phi X}\\ &\quad + 3H\dot\phi^3(4G_{3X} + \dot\phi^2G_{3XX}) - 12H(HG_4 + \dot\phi G_{4\phi}),\end{aligned} \tag{B4}$$

$$A_6 = -\dot\phi^2G_{3X} + 2G_{4\phi}, \tag{B5}$$

$$\begin{aligned}\mu &= -K_\phi + \dot\phi^2K_{\phi X} - \dot\phi^2G_{3\phi\phi} + 3H\dot\phi^3G_{3\phi X}\\ &\quad - 6H^2G_{4\phi} - 6H\dot\phi G_{4\phi\phi},\end{aligned} \tag{B6}$$

$$B_1 = 12G_4, \tag{B7}$$

$$B_2 = -3\dot{\phi}^2 G_{3X} + 6G_{4\phi}, \tag{B8}$$

$$B_3 = 12(\dot{\phi}G_{4\phi} + 3HG_4), \tag{B9}$$

$$B_4 = 3[\dot{\phi}K_X - 2\dot{\phi}G_{3\phi} - 2\dot{\phi}\,\ddot{\phi}\,G_{3X} - \dot{\phi}^3(G_{3\phi X} + \ddot{\phi}G_{3XX}) + 4HG_{4\phi} + 4\dot{\phi}G_{4\phi\phi}], \tag{B10}$$

$$B_5 = 3(\dot{\phi}^3 G_{3X} - 4HG_4 - 2\dot{\phi}G_{4\phi}), \tag{B11}$$

$$B_6 = 4G_4, \qquad B_7 = 4G_{4\phi}, \qquad B_8 = 4G_4, \tag{B12}$$

$$B_9 = -3K_X\dot{\phi}^2 + 6G_{3\phi}\dot{\phi}^2 + 3G_{3\phi X}\dot{\phi}^4 + 12G_{3X}\dot{\phi}^2\ddot{\phi} + 3G_{3XX}\dot{\phi}^4\ddot{\phi} - 36G_4H^2 - 24G_4\dot{H} - 24G_{4\phi}H\dot{\phi} - 12G_{4\phi\phi}\dot{\phi}^2 - 12G_{4\phi}\ddot{\phi}, \tag{B13}$$

and using Eq. (68) to eliminate G_4 in favor of K we can express B_9 as

$$B_9 = 3(2K - \dot{\phi}^2 K_X + 2\dot{\phi}^2\ddot{\phi}G_{3X} + \dot{\phi}^4 G_{3\phi X} + \dot{\phi}^4\ddot{\phi}G_{3XX}), \tag{B14}$$

$$\nu = K_\phi - \dot{\phi}^2(G_{3\phi\phi} + \ddot{\phi}G_{3\phi X}) + 2(3H^2 + 2\dot{H})G_{4\phi} + 2(\ddot{\phi} + 2H\dot{\phi})G_{4\phi\phi} + 2\dot{\phi}^2 G_{4\phi\phi\phi}, \tag{B15}$$

$$C_1 = 4G_4, \tag{B16}$$

$$C_2 = -\dot{\phi}^2 G_{3X} + 2G_{4\phi}, \tag{B17}$$

$$C_3 = \dot{\phi}^3 G_{3X} - 4HG_4 - 2\dot{\phi}G_{4\phi}, \tag{B18}$$

$$C_4 = \dot{\phi}(K_X - 2G_{3\phi} + 2G_{4\phi\phi}) + H(3\dot{\phi}^2 G_{3X} - 2G_{4\phi}), \tag{B19}$$

$$D_1 = -3(\dot{\phi}^2 G_{3X} - 2G_{4\phi}), \tag{B20}$$

$$D_2 = -K_X - \dot{\phi}^2 K_{XX} + 2G_{3\phi} - 6H\dot{\phi}G_{3X} + \dot{\phi}^2 G_{3\phi X} - 3H\dot{\phi}^3 G_{3XX}, \tag{B21}$$

$$D_3 = -3(\dot{\phi}K_X - 2\dot{\phi}G_{3\phi} + 6H\dot{\phi}^2 G_{3X} + 2\dot{\phi}\,\ddot{\phi}\,G_{3X} + \dot{\phi}^3 G_{3\phi X} + \dot{\phi}^3\ddot{\phi}G_{3XX} - 8HG_{4\phi}), \tag{B22}$$

$$\begin{aligned} D_4 &= \frac{d}{dt}D_2 + 3HD_2 \\ &= -3HK_X - K_{\phi X}\dot{\phi} - K_{\phi XX}\dot{\phi}^3 - K_{XXX}\dot{\phi}^3\ddot{\phi} - 3K_{XX}(H\dot{\phi}^2 + \dot{\phi}\,\ddot{\phi}) + 6HG_{3\phi} + 2G_{3\phi\phi}\dot{\phi} - 6G_{3X}(3H^2\dot{\phi} + \dot{H}\,\dot{\phi} + H\ddot{\phi}) \\ &\quad + G_{3\phi X}(-3H\dot{\phi}^2 + 4\dot{\phi}\,\ddot{\phi}) + G_{3\phi\phi X}\dot{\phi}^3 - 3G_{3XX}\dot{\phi}^2(3H^2\dot{\phi} + \dot{H}\,\dot{\phi} + 5H\ddot{\phi}) + G_{\phi XX}(H\dot{\phi}^3\ddot{\phi} - 3H\dot{\phi}^4) - 3G_{3XXX}H\dot{\phi}^4\ddot{\phi}, \end{aligned} \tag{B23}$$

$$D_5 = \dot{\phi}(K_X + \dot{\phi}_{XX}^2 - 2G_{3\phi} - \dot{\phi}^2 G_{3\phi X}) + 3H(3\dot{\phi}^2 G_{3X} + \dot{\phi}^4 G_{3XX} - 2G_{4\phi}), \tag{B24}$$

$$D_7 = 4G_{4\phi}, \tag{B25}$$

$$\begin{aligned} D_8 &= 9H\dot{\phi}^{-1}K + 3K_\phi - 3(\ddot{\phi} + 3H\dot{\phi})K_X - 3\dot{\phi}^2(K_{\phi X} + \ddot{\phi}K_{XX}) + 3(2\ddot{\phi} + 3H\dot{\phi})G_{3\phi} \\ &\quad - 9\dot{\phi}(3H\ddot{\phi} + 3H^2\dot{\phi} + \dot{H}\,\dot{\phi})G_{3X} + 3\dot{\phi}^2 G_{3\phi\phi} + 3\dot{\phi}^2(\ddot{\phi} - 3H\dot{\phi})G_{3\phi X} - 9H\dot{\phi}^3\ddot{\phi}G_{3XX} \\ &\quad + 18H\dot{\phi}^{-1}(3H^2 + 2\dot{H})G_4 + 18\dot{\phi}^{-1}(H\ddot{\phi} + 4H^2\dot{\phi} + \dot{H}\,\dot{\phi})G_{4\phi} + 18H\dot{\phi}G_{4\phi\phi}, \end{aligned} \tag{B26}$$

and using Eqs. (68) and (74) we find that

$$D_8 = 0, \tag{B27}$$

$$D_9 = -K_X + 2G_{3\phi} - 4H\dot{\phi}G_{3X} - \ddot{\phi}(2G_{3X} + \dot{\phi}^2 G_{3XX}) - \dot{\phi}^2 G_{3\phi X}, \tag{B28}$$

$$D_{10} = -\dot{\phi}^2 G_{3X} + 2G_{4\phi}, \tag{B29}$$

$$D_{11} = K_\phi + (\ddot{\phi} + 3H\dot{\phi})K_X + \dot{\phi}^2(4\ddot{\phi} + 3H\dot{\phi})K_{XX} + \dot{\phi}^4(K_{\phi XX} + \ddot{\phi}K_{XXX}) - 2(\ddot{\phi} + 3H\dot{\phi})G_{3\phi} + 9\dot{\phi}(2H\ddot{\phi} + 3H^2\dot{\phi} + \dot{H}\dot{\phi})G_{3X} - \dot{\phi}^2 G_{3\phi\phi} - \dot{\phi}^2(5\ddot{\phi} - 3H\dot{\phi})G_{3\phi X} - \dot{\phi}^4 G_{3\phi\phi X} + 3\dot{\phi}^3(7H\ddot{\phi} + 3H^2\dot{\phi} + \dot{H}\dot{\phi})G_{3XX} - \dot{\phi}^4(\ddot{\phi} - 3H\dot{\phi})G_{3\phi XX} + 3H\dot{\phi}^5\ddot{\phi}G_{3XXX} - 6(2H^2 + \dot{H})G_{4\phi}, \tag{B30}$$

$$M^2 = -K_{\phi\phi} + (\ddot{\phi} + 3H\dot{\phi})K_{\phi X} + \dot{\phi}^2 K_{\phi\phi X} + \dot{\phi}^2\ddot{\phi}K_{\phi XX} - \ddot{\phi}[2G_{3\phi\phi} + \dot{\phi}^2 G_{3\phi\phi X} - 3H\dot{\phi}(2G_{3\phi X} + \dot{\phi}^2 G_{3\phi XX})] - 6H\dot{\phi}G_{3\phi\phi} + 3\dot{\phi}^2(3H^2 + \dot{H})G_{3\phi X} - \dot{\phi}^2 G_{3\phi\phi\phi} + 3H\dot{\phi}^3 G_{3\phi\phi X} - 6(2H^2 + \dot{H})G_{4\phi\phi}. \tag{B31}$$

For the DE effective perturbation equations we found the following coefficients:

$$\mathcal{F}_1 = (A_6 - B_7)B_7 G_4 G_{4\phi}^2(B_7 G_4 - (B_6 - 2)G_{4\phi}), \tag{B32}$$

$$\mathcal{F}_2 = (A_6 - B_7)B_7 G_4(3\nu G_{4\phi}^2 + 2B_2 G_{4\phi\phi}^2\dot{\phi}^2 - G_{4\phi}(B_4 G_{4\phi\phi}\dot{\phi} + B_2 G_{4\phi\phi\phi}\dot{\phi}^2 + B_2 G_{4\phi\phi}\ddot{\phi})) + G_{4\phi}^2(B_2 B_7(B_7 - A_6)G_{4\phi\phi}\dot{\phi}^2 + G_{4\phi}(B_9(B_7^2 - 2D_9) + (A_6 - B_7)B_7(B_4\dot{\phi} + B_2\ddot{\phi}))), \tag{B33}$$

$$\mathcal{F}_3 = B_6 B_9 M^2 G_{4\phi}^3, \tag{B34}$$

$$\mathcal{F}_4 = G_{4\phi}, \tag{B35}$$

$$\mathcal{F}_5 = B_6(A_6^2 - 2A_6 B_7 + B_6 D_9)G_{4\phi}^2, \tag{B36}$$

$$\mathcal{F}_6 = -B_6^2 M^2 G_{4\phi}^2, \tag{B37}$$

$$\mathcal{F}_7 = G_{4\phi}(A_6(A_6 - B_7)B_7 G_4 + (B_6 - 2)(B_6 D_9 - A_6 B_7)G_{4\phi}), \tag{B38}$$

$$\mathcal{F}_8 = (G_{4\phi}^2(A_4(B_7^2 - B_6 D_9) - (B_6 - 2)B_6 M^2 + 6(B_7^2 - B_6 D_9)H^2 + A_2(A_6 - B_7)B_7\dot{\phi}) - (A_6 - B_7)B_7 G_4(\mu G_{4\phi} + A_2 G_{4\phi\phi}\dot{\phi})), \tag{B39}$$

$$\mathcal{F}_9 = B_6 M^2 G_{4\phi}^2(A_4 + 6H^2), \tag{B40}$$

$$\mathcal{F}_{10} = G_{4\phi}((A_6 - B_7)B_7 C_4 G_4 + (B_7^2 - B_6 D_9)G_{4\phi}(C_3 + 2H)) + (A_6 - B_7)B_7 C_2(G_{4\phi}^2 - G_4 G_{4\phi\phi})\dot{\phi}, \tag{B41}$$

$$\mathcal{F}_{11} = B_6 M^2 G_{4\phi}^2(C_3 + 2H). \tag{B42}$$

The coefficients for the KGB DE effective perturbation equations are

$$\hat{\mathcal{F}}_2 = -B_9 D_9 + 3A_6\nu - 6D_9(3H^2 + 2\dot{H}), \tag{B43}$$

$$\hat{\mathcal{F}}_3 = M^2(B_9 + 18H^2 + 12\dot{H}), \tag{B44}$$

$$\hat{\mathcal{F}}_5 = A_6^2 + B_6 D_9, \tag{B45}$$

$$\hat{\mathcal{F}}_6 = -B_6 M^2, \tag{B46}$$

$$\hat{\mathcal{F}}_7 = -A_6^2 - (B_6 - 2)D_9, \tag{B47}$$

$$\hat{\mathcal{F}}_8 = A_4 D_9 + M^2(B_6 - 2) + A_6\mu + 6D_9 H^2, \tag{B48}$$

$$\hat{\mathcal{F}}_9 = -M^2(A_4 + 6H^2), \tag{B49}$$

$$\hat{\mathcal{F}}_{10} = M^2(C_3 + 2H), \tag{B50}$$

$$\hat{\mathcal{F}}_{11} = A_6 C_4 - C_3 D - 9 - 2D_9 H. \tag{B51}$$

[1] A. G. Riess *et al.* (Supernova Search Team), Astron. J. **116**, 1009 (1998).
[2] S. Perlmutter *et al.* (Supernova Cosmology Project), Astrophys. J. **517**, 565 (1999).
[3] J. T. Nielsen, A. Guffanti, and S. Sarkar, Sci. Rep. **6**, 35596 (2016).
[4] A. G. Riess *et al.*, Astrophys. J. **659**, 98 (2007).
[5] M. Betoule *et al.* (SDSS Collaboration), Astron. Astrophys. **568**, A22 (2014).
[6] N. Aghanim *et al.* (Planck Collaboration), arXiv:1807.06209.
[7] T. M. C. Abbott *et al.* (DES Collaboration), Phys. Rev. D **98**, 043526 (2018).

[8] A. Heavens, Y. Fantaye, E. Sellentin, H. Eggers, Z. Hosenie, S. Kroon, and A. Mootoovaloo, Phys. Rev. Lett. **119**, 101301 (2017).
[9] G. Bertone and D. Hooper, Rev. Mod. Phys. **90**, 045002 (2018).
[10] S. Weinberg, Rev. Mod. Phys. **61**, 1 (1989).
[11] S. M. Carroll, Living Rev. Relativity **4**, 1 (2001).
[12] L. Kofman and A. A. Starobinsky, Pisma Astron. Zh. **11**, 643 (1985) [Sov. Astron. Lett. **11**, 271 (1985)].
[13] T. Clifton, P. G. Ferreira, A. Padilla, and C. Skordis, Phys. Rep. **513**, 1 (2012).
[14] E. Bertschinger, Phil. Trans. R. Soc. A **369**, 4947 (2011).
[15] B. Bertotti, L. Iess, and P. Tortora, Nature (London) **425**, 374 (2003).
[16] R. Reyes, R. Mandelbaum, U. Seljak, T. Baldauf, J. E. Gunn, L. Lombriser, and R. E. Smith, Nature (London) **464**, 256 (2010).
[17] T. E. Collett, L. J. Oldham, R. J. Smith, M. W. Auger, K. B. Westfall, D. Bacon, R. C. Nichol, K. L. Masters, K. Koyama, and R. van den Bosch, Science **360**, 1342 (2018).
[18] B. P. Abbott, R. Abbott, T. D. Abbott, M. R. Abernathy, F. Acernese, K. Ackley, C. Adams, T. Adams, P. Addesso, R. X. Adhikari *et al.* (LIGO Scientific and Virgo Collaborations), Phys. Rev. Lett. **116**, 221101 (2016).
[19] J.-h. He, L. Guzzo, B. Li, and C. M. Baugh, Nat. Astron. **2**, 967 (2018).
[20] P. Delva, N. Puchades, E. Schönemann, F. Dilssner, C. Courde, S. Bertone, F. Gonzalez, A. Hees, C. Le Poncin-Lafitte, F. Meynadier *et al.*, Phys. Rev. Lett. **121**, 231101 (2018).
[21] S. Herrmann, F. Finke, M. Lülf, O. Kichakova, D. Puetzfeld, D. Knickmann, M. List, B. Rievers, G. Giorgi, C. Günther *et al.*, Phys. Rev. Lett. **121**, 231102 (2018).
[22] M. Ishak, Living Rev. Relativity **22**, 1 (2019).
[23] C. A. Luna, S. Basilakos, and S. Nesseris, Phys. Rev. D **98**, 023516 (2018).
[24] S. Basilakos, S. Nesseris, F. K. Anagnostopoulos, and E. N. Saridakis, J. Cosmol. Astropart. Phys. 08 (2018) 008.
[25] J. Perez-Romero and S. Nesseris, Phys. Rev. D **97**, 023525 (2018).
[26] S. Basilakos and S. Nesseris, Phys. Rev. D **96**, 063517 (2017).
[27] S. Nesseris, G. Pantazis, and L. Perivolaropoulos, Phys. Rev. D **96**, 023542 (2017).
[28] S. Basilakos and S. Nesseris, Phys. Rev. D **94**, 123525 (2016).
[29] E. J. Copeland, M. Sami, and S. Tsujikawa, Int. J. Mod. Phys. D **15**, 1753 (2006).
[30] B. Ratra and P. J. E. Peebles, Phys. Rev. D **37**, 3406 (1988).
[31] C. Armendariz-Picon, V. F. Mukhanov, and P. J. Steinhardt, Phys. Rev. Lett. **85**, 4438 (2000).
[32] M. Kunz and D. Sapone, Phys. Rev. Lett. **98**, 121301 (2007).
[33] L. Pogosian, A. Silvestri, K. Koyama, and G.-B. Zhao, Phys. Rev. D **81**, 104023 (2010).
[34] S. Capozziello, S. Nojiri, and S. D. Odintsov, Phys. Lett. B **634**, 93 (2006).
[35] S. Capozziello, S. Nojiri, S. D. Odintsov, and A. Troisi, Phys. Lett. B **639**, 135 (2006).
[36] S. Capozziello, C. A. Mantica, and L. G. Molinari, Int. J. Geom. Methods Mod. Phys. **16**, 1950008 (2019).
[37] T. Multamaki and I. Vilja, Phys. Rev. D **73**, 024018 (2006).
[38] A. de la Cruz-Dombriz and A. Dobado, Phys. Rev. D **74**, 087501 (2006).
[39] L. Pogosian and A. Silvestri, Phys. Rev. D **77**, 023503 (2008); **81**, 049901(E) (2010).
[40] S. Nesseris, Phys. Rev. D **88**, 123003 (2013).
[41] S. Nesseris and A. Shafieloo, Mon. Not. R. Astron. Soc. **408**, 1879 (2010).
[42] S. Nesseris and J. Garcia-Bellido, J. Cosmol. Astropart. Phys. 11 (2012) 033.
[43] S. Tsujikawa, Phys. Rev. D **76**, 023514 (2007).
[44] G. W. Horndeski, Int. J. Theor. Phys. **10**, 363 (1974).
[45] T. Baker, P. G. Ferreira, and C. Skordis, Phys. Rev. D **87**, 024015 (2013).
[46] P. Creminelli and F. Vernizzi, Phys. Rev. Lett. **119**, 251302 (2017).
[47] J. Sakstein and B. Jain, Phys. Rev. Lett. **119**, 251303 (2017).
[48] J. M. Ezquiaga and M. Zumalacarregui, Phys. Rev. Lett. **119**, 251304 (2017).
[49] T. Baker, E. Bellini, P. G. Ferreira, M. Lagos, J. Noller, and I. Sawicki, Phys. Rev. Lett. **119**, 251301 (2017).
[50] L. Amendola, M. Kunz, I. D. Saltas, and I. Sawicki, Phys. Rev. Lett. **120**, 131101 (2018).
[51] M. Crisostomi and K. Koyama, Phys. Rev. D **97**, 084004 (2018).
[52] N. Frusciante, S. Peirone, S. Casas, and N. A. Lima, Phys. Rev. D **99**, 063538 (2019).
[53] R. Kase and S. Tsujikawa, Int. J. Mod. Phys. D **28**, 1942005 (2019).
[54] R. McManus, L. Lombriser, and J. Pearrubia, J. Cosmol. Astropart. Phys. 11 (2016) 006.
[55] L. Lombriser and A. Taylor, J. Cosmol. Astropart. Phys. 03 (2016) 031.
[56] E. J. Copeland, M. Kopp, A. Padilla, P. M. Saffin, and C. Skordis, Phys. Rev. Lett. **122**, 061301 (2019).
[57] J. Noller and A. Nicola, arXiv:1811.03082.
[58] C. de Rham and S. Melville, Phys. Rev. Lett. **121**, 221101 (2018).
[59] B. P. Abbott *et al.* (Virgo and LIGO Scientific Collaborations), Phys. Rev. Lett. **119**, 141101 (2017).
[60] T. P. Sotiriou and V. Faraoni, Rev. Mod. Phys. **82**, 451 (2010).
[61] A. De Felice and S. Tsujikawa, Living Rev. Relativity **13**, 3 (2010).
[62] S. Nojiri, S. D. Odintsov, and V. K. Oikonomou, Phys. Rep. **692**, 1 (2017).
[63] S. Nojiri and S. D. Odintsov, Phys. Rep. **505**, 59 (2011).
[64] C. Deffayet, O. Pujolas, I. Sawicki, and A. Vikman, J. Cosmol. Astropart. Phys. 10 (2010) 026.
[65] R. Arjona, W. Cardona, and S. Nesseris, Phys. Rev. D **99**, 043516 (2019).
[66] M. Kunz and D. Sapone, Phys. Rev. D **74**, 123503 (2006).
[67] D. Blas, J. Lesgourgues, and T. Tram, J. Cosmol. Astropart. Phys. 07 (2011) 034.
[68] R. A. Battye, B. Bolliet, and J. A. Pearson, Phys. Rev. D **93**, 044026 (2016).
[69] R. A. Battye, B. Bolliet, and F. Pace, Phys. Rev. D **97**, 104070 (2018).
[70] M. Zumalacarregui, E. Bellini, I. Sawicki, J. Lesgourgues, and P. G. Ferreira, J. Cosmol. Astropart. Phys. 08 (2017) 019.

[71] D. W. Hogg, D. J. Eisenstein, M. R. Blanton, N. A. Bahcall, J. Brinkmann, J. E. Gunn, and D. P. Schneider, Astrophys. J. **624**, 54 (2005).
[72] P. A. R. Ade *et al.* (Planck Collaboration), Astron. Astrophys. **594**, A16 (2016).
[73] T. Kobayashi, M. Yamaguchi, and J. Yokoyama, Prog. Theor. Phys. **126**, 511 (2011).
[74] T. Chiba, Phys. Lett. B **575**, 1 (2003).
[75] C. Brans and R. H. Dicke, Phys. Rev. **124**, 925 (1961).
[76] I. Quiros, Int. J. Mod. Phys. D **28**, 1930012 (2019).
[77] Q. Fang, S. Chen, and J. Jing, Int. J. Mod. Phys. D **28**, 1950112 (2019).
[78] M. Kopp, C. Skordis, D. B. Thomas, and S. Ilić, Phys. Rev. Lett. **120**, 221102 (2018).
[79] R. Kimura and K. Yamamoto, J. Cosmol. Astropart. Phys. 04 (2011) 025.
[80] A. De Felice, T. Kobayashi, and S. Tsujikawa, Phys. Lett. B **706**, 123 (2011).
[81] J. Matsumoto, J. Cosmol. Astropart. Phys. 01 (2019) 054.
[82] W. Cardona, L. Hollenstein, and M. Kunz, J. Cosmol. Astropart. Phys. 07 (2014) 032.
[83] L. Amendola and S. Tsujikawa, *Dark Energy* (Cambridge University Press, Cambridge, England, 2015).
[84] R. J. Scherrer, Phys. Rev. Lett. **93**, 011301 (2004).
[85] R. de Putter and E. V. Linder, Astropart. Phys. **28**, 263 (2007).
[86] O. Pujolas, I. Sawicki, and A. Vikman, J. High Energy Phys. 11 (2011) 156.
[87] J. M. Ezquiaga and M. Zumalacarregui, Front. Astron. Space Sci. **5**, 44 (2018).
[88] B. Sagredo, S. Nesseris, and D. Sapone, Phys. Rev. D **98**, 083543 (2018).
[89] Y.-S. Song, W. Hu, and I. Sawicki, Phys. Rev. D **75**, 044004 (2007).
[90] S. Dodelson, *Modern Cosmology* (Academic Press, Amsterdam, 2003).
[91] D. M. Scolnic *et al.*, Astrophys. J. **859**, 101 (2018).
[92] F. Beutler, C. Blake, M. Colless, D. H. Jones, L. Staveley-Smith, L. Campbell, Q. Parker, W. Saunders, and F. Watson, Mon. Not. R. Astron. Soc. **416**, 3017 (2011).
[93] L. Anderson *et al.* (BOSS Collaboration), Mon. Not. R. Astron. Soc. **441**, 24 (2014).
[94] X. Xu, N. Padmanabhan, D. J. Eisenstein, K. T. Mehta, and A. J. Cuesta, Mon. Not. R. Astron. Soc. **427**, 2146 (2012).
[95] C. Blake *et al.*, Mon. Not. R. Astron. Soc. **425**, 405 (2012).
[96] A. J. Ross, L. Samushia, C. Howlett, W. J. Percival, A. Burden, and M. Manera, Mon. Not. R. Astron. Soc. **449**, 835 (2015).
[97] H. Gil-Marin *et al.*, Mon. Not. R. Astron. Soc. **460**, 4210 (2016).
[98] T. M. C. Abbott *et al.* (DES Collaboration), Mon. Not. R. Astron. Soc. **483**, 4866 (2019).
[99] Z. Zhai and Y. Wang, J. Cosmol. Astropart. Phys. 07 (2019) 005.
[100] E. Gaztanaga, A. Cabre, and L. Hui, Mon. Not. R. Astron. Soc. **399**, 1663 (2009).
[101] R. Jimenez and A. Loeb, Astrophys. J. **573**, 37 (2002).
[102] M. Moresco, L. Pozzetti, A. Cimatti, R. Jimenez, C. Maraston, L. Verde, D. Thomas, A. Citro, R. Tojeiro, and D. Wilkinson, J. Cosmol. Astropart. Phys. 05 (2016) 014.
[103] R.-Y. Guo and X. Zhang, Eur. Phys. J. C **76**, 163 (2016).
[104] C. Zhang, H. Zhang, S. Yuan, T.-J. Zhang, and Y.-C. Sun, Res. Astron. Astrophys. **14**, 1221 (2014).
[105] D. Stern, R. Jimenez, L. Verde, M. Kamionkowski, and S. A. Stanford, J. Cosmol. Astropart. Phys. 02 (2010) 008.
[106] M. Moresco *et al.*, J. Cosmol. Astropart. Phys. 08 (2012) 006.
[107] C.-H. Chuang and Y. Wang, Mon. Not. R. Astron. Soc. **435**, 255 (2013).
[108] M. Moresco, Mon. Not. R. Astron. Soc. **450**, L16 (2015).
[109] T. Delubac *et al.* (BOSS Collaboration), Astron. Astrophys. **574**, A59 (2015).
[110] W. J. Percival and M. White, Mon. Not. R. Astron. Soc. **393**, 297 (2009).
[111] Y.-S. Song and W. J. Percival, J. Cosmol. Astropart. Phys. 10 (2009) 004.
[112] S. Nesseris and L. Perivolaropoulos, J. Cosmol. Astropart. Phys. 01 (2007) 018.
[113] L. Kazantzidis and L. Perivolaropoulos, Phys. Rev. D **97**, 103503 (2018).
[114] L. Amendola, V. Marra, and M. Quartin, Mon. Not. R. Astron. Soc. **430**, 1867 (2013).
[115] D. Huterer, D. Shafer, D. Scolnic, and F. Schmidt, J. Cosmol. Astropart. Phys. 05 (2017) 015.
[116] S. J. Turnbull, M. J. Hudson, H. A. Feldman, M. Hicken, R. P. Kirshner, and R. Watkins, Mon. Not. R. Astron. Soc. **420**, 447 (2012).
[117] M. J. Hudson and S. J. Turnbull, Astrophys. J. **751**, L30 (2012).
[118] M. Davis, A. Nusser, K. Masters, C. Springob, J. P. Huchra, and G. Lemson, Mon. Not. R. Astron. Soc. **413**, 2906 (2011).
[119] M. Feix, A. Nusser, and E. Branchini, Phys. Rev. Lett. **115**, 011301 (2015).
[120] C. Howlett, A. Ross, L. Samushia, W. Percival, and M. Manera, Mon. Not. R. Astron. Soc. **449**, 848 (2015).
[121] C. Blake *et al.*, Mon. Not. R. Astron. Soc. **436**, 3089 (2013).
[122] L. Samushia, W. J. Percival, and A. Raccanelli, Mon. Not. R. Astron. Soc. **420**, 2102 (2012).
[123] A. G. Sanchez *et al.*, Mon. Not. R. Astron. Soc. **440**, 2692 (2014).
[124] C.-H. Chuang *et al.*, Mon. Not. R. Astron. Soc. **461**, 3781 (2016).
[125] A. Pezzotta *et al.*, Astron. Astrophys. **604**, A33 (2017).
[126] T. Okumura *et al.*, Publ. Astron. Soc. Jpn. **68**, 38 (2016).
[127] G.-B. Zhao *et al.*, Mon. Not. R. Astron. Soc. **482**, 3497 (2019).
[128] H. Akaike, IEEE Trans. Autom. Control **19**, 716 (1974).
[129] A. R. Liddle, Mon. Not. R. Astron. Soc. **377**, L74 (2007).
[130] S. Nesseris and J. Garcia-Bellido, J. Cosmol. Astropart. Phys. 08 (2013) 036.
[131] L. Perenon, J. Bel, R. Maartens, and A. de la Cruz-Dombriz, J. Cosmol. Astropart. Phys. 06 (2019) 020.
[132] J. Noller and A. Nicola, Phys. Rev. D **99**, 103502 (2019).
[133] A. Spurio Mancini, F. Kohlinger, B. Joachimi, V. Pettorino, B. M. Schafer, R. Reischke, S. Brieden, M. Archidiacono, and J. Lesgourgues, arXiv:1901.03686.
[134] R. Courant and D. Hilbert, *Methods of Mathematical Physics vol. 1* (Interscience Publishers Inc., New York, 1953), p. 106.